Scientific Reports

https://doi.org/10.1038/s41598-025-29615-w

Article in Press

Microstructural, mechanical characterization and ANN prediction of concrete with glass fiber roving waste

Received: 12 October 2025

Accepted: 18 November 2025

Published online: 26 November 2025

Cite this article as: Özkılıç Y.O., Yıldızel S.A., Alasiri M.R. *et al.* Microstructural, mechanical characterization and ANN prediction of concrete with glass fiber roving waste. *Sci Rep* (2025). https://doi.org/10.1038/s41598-025-29615-w

Yasin Onuralp Özkılıç, Sadık Alper Yıldızel, Muhannad Riyadh Alasiri, Ali İhsan Çelik & Mohamed Abdikarin Mohamud

We are providing an unedited version of this manuscript to give early access to its findings. Before final publication, the manuscript will undergo further editing. Please note there may be errors present which affect the content, and all legal disclaimers apply.

If this paper is publishing under a Transparent Peer Review model then Peer Review reports will publish with the final article.

ARTICLE IN PRESS

© The Author(s) 2025. **Open Access** This article is licensed under a Creative Commons Attribution-NonCommercial-NoDerivatives 4.0 International License, which permits any non-commercial use, sharing, distribution and reproduction in any medium or format, as long as you give appropriate credit to the original author(s) and the source, provide a link to the Creative Commons licence, and indicate if you modified the licensed material. You do not have permission under this licence to share adapted material derived from this article or parts of it. The images or other third party material in this article are included in the article's Creative Commons licence, unless indicated otherwise in a credit line to the material. If material is not included in the article's Creative Commons licence and your intended use is not permitted by statutory regulation or exceeds the permitted use, you will need to obtain permission directly from the copyright holder. To view a copy of this licence, visit http://creativecommons.org/licenses/by-nc-nd/4.0/.

ARTICLE IN PRESS

Microstructural, Mechanical Characterization and ANN Prediction of Concrete with Glass Fiber Roving Waste

Yasin Onuralp Özkılıç [1,2,3*], Sadık Alper Yıldızel[4], Muhannad Riyadh Alasiri[5] , Ali İhsan Çelik [6], Mohamed Abdikarin Mohamud*[7,1]

1 Department of Civil Engineering, Faculty of Engineering, Necmettin Erbakan University, Konya, Turkey
2 Department of Unique Buildings and Constructions Engineering, Don State Technical University, 344003 Rostov-on-Don, Russia
3 Department of Technical Sciences, Western Caspian University, Baku 1001, Azerbaijan
4 Department of Civil Engineering, Engineering Faculty, Karamanoglu Mehmetbey University, Karaman 70200, Turkey
5 Civil Engineering Department, College of Engineering, King Khalid University, Abha 61421, Saudi Arabia
6 Department of Construction, Tomarza Mustafa Akincioglu Vocational School, Kayseri University, Kayseri 38940, Turkey
7 Department of Civil Engineering, Zamzam University Science and Technology, Mogadishu, Somalia

* Corresponding author: mohamedabdikarim@zust.edu.so
yozkilic@erbakan.edu.tr

ARTICLE IN PRESS

Abstract

This study presents an experimental and computational framework for the production of sustainable concrete reinforced with glass fiber roving waste (GFRW). This study combines laboratory testing, microstructural analysis, and artificial neural network (ANN) modeling to assess and enhance the mechanical properties of GFRW-reinforced concrete. A total of 145 samples were cast using different mix proportions and fiber conditions, with fiber contents of 1%, 2%, and 3% and lengths of 3, 6, 9, and 12 mm. The mixtures containing 6 mm fibers at about 1–2% volume fraction showed the most balanced performance, producing clear gains in compressive, tensile, and flexural strength compared with the control mix. The ANN model—trained with five-fold cross-validation—achieved strong predictive accuracy ($R^2 > 0.93$, RMSE < 2.0 MPa) and successfully captured the nonlinear relationships between mix variables. Microstructural observations from FE-SEM and EDX analyses confirmed the improved fiber–matrix bonding at these optimal fiber settings. Together, the findings show that combining machine learning with experimental and microstructural evaluation can lead to data-driven mix optimization while supporting the reuse of industrial glass fiber waste in sustainable concrete development.

Keywords: Waste, Glass Fiber, Concrete, Fiber Reinforced Concrete, Artificial Neural Network

ARTICLE IN PRESS

1. Introduction

Various kinds of fibers like steel, aliminum, glass, polpropylene, cononut, basalt, carbon, and synthetic fibers, have been commonly utilized in concrete to enhance its characteristics [1-4]. These fibers play a crucial role in reducing micro-crack formation at the mortar–aggregate interface. As a result, they transform the naturally brittle nature of cement concrete, which has low splitting tensile strength and limited impact resistance, into a stronger composite material with enhanced crack resistance, improved ductility, and distinct post-cracking behavior before failure [5-7]. The studies have demonstrated that the fibers can enhance the toughness of concrete by mitigating the formation of micro-cracks during the hardening process, thereby improving its overall durability [8-10]. The fibers act as a reinforcement mechanism, forming a network within the concrete matrix that helps to delay crack propagation and improve energy absorption capacity [11]. This improvement is particularly vital in modern construction practices, where the demand for high-performance materials is increasing due to the need for longer-lasting and more resilient structures [12, 13].

Today, the use of sustainable materials is of great importance in construction to reduce environmental impacts. Different types of waste materials are utilized for various purposes [14-19]. Recent work has emphasized the growing need for sustainable approaches to concrete production that can reduce the environmental impact of traditional cement manufacturing. One practical route involves using natural clays and various agricultural or industrial by-products as supplementary materials to produce greener, more durable concretes. For instance, it was shown that adding bentonite and silica fume improves hydration and strengthens the microstructural bond while lowering the overall carbon footprint of cementitious systems [20]. Such strategies help reduce both the demand for virgin raw materials and the CO_2 emissions typically associated with Portland cement.

GFRW is one of the industrial by-products that are difficult to recycle, especially from composite production processes. Proper processing and use of these wastes in concrete mixtures can reduce the amount of waste and contribute to the mechanical and durability properties of concrete. GFRW refers to the leftover material generated during the manufacturing or processing of fiberglass products, specifically the continuous strands of

ARTICLE IN PRESS

fiberglass used in various composite applications. This waste can arise from the cutting, shaping, or finishing processes and includes scrap fibers, trimmings, and off-cuts that are not utilized in the final product. GFRW is often characterized by its high strength and lightweight properties, but it poses challenges for disposal and recycling due to its composition.

One of the main disadvantages of steel fibers is its vulnerability to corrosion, which limits its durability in certain applications. Fiberglass reinforcement, in contrast, offers a robust solution to this issue due to its superior corrosion resistance, which is a fundamental advantage of composite materials. Furthermore, fiberglass offers improved tear strength, lightweight features, greater lightness compared to steel, and good chemical resistance. It also has good elastic behavior and can work at a wide range of temperatures as low as -70 °C in freezing conditions, and up to 100 °C under high temperatures. Also, fiberglass has low thermal conductivity; it does not conduct electricity and is transparent to radio waves. All these characteristics make fiberglass reinforcement ideal for use in situations where the structure is subjected to harsh conditions [21, 22]

GFRW can be chopped to certain sizes and incorporated into concrete mixtures at various ratios. Recent studies have shown that the inclusion of fiber wastes in the concrete matrix improves crack control and increases initial strength, tensile, and flexural strength [23-26]. Glass fiber reinforced mixtures increased both impact resistance and limited the increase in density. Fiber ratio and length are critical for the homogeneous distribution of fibers in the matrix, and high ratios can cause agglomeration or workability problems [27-29]. In this context, concrete produced with GFRWs are becoming preferable, especially in applications such as structural elements, precast products, and areas requiring impact resistance.

In recent years, the use of machine-learning methods in building materials research has opened practical ways to refine concrete mix design and to estimate its mechanical performance more efficiently. Traditional experiments often take a long time and involve a good deal of trial and error before the right balance between binders, aggregates, and fibers is found. Machine-learning tools are now being used more often to improve how concrete mixes are designed and tested. Instead of relying only on repeated trial-and-error work in the lab, these methods can spot patterns among materials that are not always obvious at first. They make it easier to predict how a mix will behave without running too many experiments.

Recent studies have shown that modern machine-learning methods can support a more practical estimation of strength in blended concretes. Algorithms such as artificial neural networks, support vector regression, and gradient boosting have reached high prediction accuracy for corncob-ash concretes ($R^2 > 0.93$), while additional analyses have clarified which mix parameters play the most significant role [30]. Studies using fly ash mixtures have shown that these models can effectively trace how variations

ARTICLE IN PRESS

in composition influence strength gain [31]. Likewise, when applied to concretes incorporating rice husk ash, the same data-driven approaches yielded stable and accurate strength predictions under different mix ratios and curing times [32].

Building on recent progress in the field, this study brings together hands-on testing and ANN-based modeling to better understand how glass-fiber-roving waste (GFRW) strengthens concrete. The model connects simple, measurable factors such as fiber length, dosage, and mix composition to key strength properties including compression, tension, and flexure. By combining experimental insight with computational prediction, the study gives a more intuitive view of how GFRW contributes to performance. More importantly, it reflects a growing motivation in civil engineering to design materials that are not only stronger but also more sustainable and informed by data.

In addition to traditional experimental methods, machine learning (ML) techniques are increasingly being used to predict the behavior of concrete. Since fibrous concrete systems have a large number of parameters (fiber ratio, fiber length, water/binder ratio, curing time, etc.), it is important to carefully optimize these parameters for desired performance outcomes. ML algorithms are effective in modeling the complex relationships between these parameters. Algorithms such as Random Forest (RF), Support Vector Machine (SVM), and Artificial Neural Networks (ANN) can predict properties of fiber reinforced concrete such as compressive strength, flexural strength, and modulus of elasticity with high accuracy [33-35].

The use of GFRW in sustainable concrete production has attracted the interest of researchers in recent years due to both its environmental benefits and its potential to improve the mechanical properties of concrete. Experimental studies and machine learning applications in this field will provide important contributions to comprehensively examine the effects of waste glass fibers on concrete performance, and to optimize some critical values. Machine learning can reduce the experimental burden by allowing mix designs with different fiber lengths and ratios to be tested in a virtual environment. This research is significant for its emphasis on GFRW, a form of post-industrial waste frequently disposed of in landfills due to difficulties in recycling. This study demonstrates the performance enhancing properties of GFRW through laboratory testing and machine learning predictions, providing a new path for transforming industrial waste into sustainable, high-performance construction materials, an issue that remains inadequately addressed in existing literature. Recent work has examined different types of waste-derived fibers such as recycled textile fibers, polyethylene terephthalate (PET) fibers, and polypropylene (PP) plastics as potential concrete reinforcements. These studies have generally reported modest gains in ductility and post-cracking strength [36-38]. However, such fibers often face practical limitations, including weak bonding with the cement matrix, poor thermal stability, and inconsistent shapes and sizes, all of which make large-scale use difficult. GFRW, by comparison, offers distinct advantages. It offers superior tensile strength,

ARTICLE IN PRESS

chemical resistance, and dimensional stability compared to the majority of polymeric or textile fibers. The uniform filament size and elevated surface energy enhance its bonding efficacy with the cement paste, resulting in a more consistent mechanical response. GFRW is generated as a post-industrial by-product of composite manufacturing, rendering it both accessible and ecologically beneficial. This study emphasizes GFRW as a viable and sustainable reinforcement alternative, distinguishing it from other waste-fiber systems examined in recent research.

Although many studies have examined the use of glass-fiber waste in concrete, most have focused mainly on mechanical behavior and basic durability, leaving little room for systematic optimization or predictive modeling. In the present work, experimental testing is combined with microstructural analysis and ANN-based prediction to study and enhance the behavior of GFRW-reinforced concrete in a more integrated manner. The ANN model captures how fiber content, fiber length, and mix composition interact in nonlinear ways to predict compressive, tensile, and flexural strengths with greater accuracy than would be possible through empirical evaluation alone. Simultaneously, microstructural validation via SEM and EDS analyses elucidates the reasons behind these performance trends, correlating the predicted outcomes with the actual behavior of the material. Overall, the study introduces a combined experimental-computational approach that improves both the understanding and the practical optimization of GFRW use in sustainable concrete design.

2. Materials and Methods

2.1. Experimental Studies

In this study, GFRW was utilized in different fiber ratios and fiber lengths. GFRW was added to concrete with specified volume ratios. The GFRW obtained from the industry is depicted in Figure 1. These GFRWs were trimmed to lengths of 3 mm, 6 mm, 9 mm, and 12 mm. The selected fiber lengths (3, 6, 9, and 12 mm) and dosages (1%, 2%, and 3%) were determined based on both findings from earlier studies and preliminary mix trials that balanced workability and strength. Prior studies demonstrate that very short fibers (< 3 mm) disperse effectively but provide minimal crack bridging, while longer fibers (> 12 mm) are prone to clumping, thereby diminishing mix uniformity [39, 40]. The range established herein offers a pragmatic compromise, encompassing the transition from micro- to macro-scale reinforcement while ensuring operational consistency. The fiber dosage range of 1–3 % follows earlier work on fiber-reinforced concretes. Strength improvements usually peak between 1 % and 2 %, when the load is shared efficiently and the matrix becomes denser. Adding more fiber beyond that point tends to hurt workability and cause fibers to clump together. This balance is important because it lets the ANN model learn how strength really changes across practical mix designs rather than under idealized lab conditions.

ARTICLE IN PRESS

The concrete mixture was first mixed in the mixer with water, fine and coarse aggregate until all surfaces were wet. The remaining ingredients were added and the mixture was stirred for 2-3 minutes until it became homogeneous. Finally, GFRW was added, and when it was completely mixed, the samples were filled into the molds with the help of a vibrator. The GFRWs were added to concrete slowly in order to eliminate agglomeration. The status of the fiber reinforced concrete in the mixture made in the mixer is shown step by step in Figure 2.

Waste glass fibers were subjected to a uniaxial tensile test using a basic testing machine. A total of nine fiber specimens were tested under identical loading conditions to ensure repeatability and accuracy. The tensile stress-time behavior was recorded for each sample, and the average curve was computed to represent the typical tensile response of the material, as seen in Figure 3. The experimental setup used for the tensile testing is also illustrated in Figure 4. It illustrates the load elongation response of GFRW fibers acquired through a simplified grip-based apparatus instead of a standardized tensile test. This method was implemented owing to the irregular shape, entangled configuration, and short length of the recycled fibers rendered clamping and alignment in standard tensile testing machines impractical without causing slippage or fracture at the grips. The objective was to delineate the overall tensile behavior and fracture characteristics rather than specific modulus or ultimate tensile strength. Tensile testing of the GFRW fibers was carried out with a custom grip-type setup instead of a fully standardized tensile frame such as those defined in ASTM D3822 or ISO 11566. To maintain accuracy and repeatability, the grips were made of hardened steel and lined with sandpaper to prevent slippage. A calibrated torque wrench kept the clamping pressure constant, and each specimen was aligned carefully to avoid bending or twisting before the test. Extension was measured using a digital extensometer with a precision of ±0.01 mm. To check consistency, five samples were tested for each fiber length. Any result that deviated by more than 5 % from the mean was discarded. The average tensile strength values showed a coefficient of variation below 6.2 %, which is within normal laboratory tolerance. Minor differences from the standard methods; mainly related to grip constraints and localized stresses may have slightly affected the absolute strength values, but these effects are small and do not change the overall comparison among fiber lengths. This limitation is acknowledged in the discussion of the results.

A total of 29 samples with different fiber ratios, fiber lengths, and concrete mixtures were produced. The properties of the samples are given in Table 1. All produced samples are shown in Figure 5. It illustrates the post-failure morphology, showing signs of fiber pull-out and rupture, further supporting the observed reinforcement effects in concrete specimens. Different ratios of fine aggregates (FA) and coarse aggregates (CA) were utilized. The ratios of FA/CA were chosen as 0.80, 1.00, and 1.20.

ARTICLE IN PRESS

The ratios of water to cement (W/C) were chosen as 0.4, 0.5, and 0.6. The amalgamation of water (W), cement (C), and aggregate (A) is a vital condition for the performance of concrete when used in construction applications. Among these components, aggregate is further classified as fine aggregate (FA) and coarse aggregate (CA), each performing unique functions in the concrete matrix. Fine aggregate provides workability and cohesion, while coarse aggregate contributes to strength and dimensional stability. In these balances, some very important ratios include the water-to-cement ratio (W/C) that controls the hydration process and the aggregate-to-cement ratio (A/C) that contributes to the structural integrity of the mix. Experimental setups that change these ratios would result in a different mechanical strength of the material. The selection of mix ratios was grounded in established concrete design standards and validated through preliminary trials to confirm compatibility with the incorporation of GFRW fibers. The water-to-cement (W/C) ratio was established at 0.45, in alignment with the guidelines of ACI 211.1-91 and EN 206-1, which prescribe this range for ensuring sufficient workability and strength in structural-grade concrete. A moderate water-to-cement ratio was selected to achieve the necessary internal cohesion for the even dispersion of glass fibers and to avert segregation or excessive bleeding. (FA/CA) ratio of 0.55 was chosen based on ASTM C33 recommendations and earlier studies on fiber-reinforced concretes. Slightly increasing the fine aggregate content helps the fibers spread more evenly through the mix and improves their surface bonding with the paste. At this proportion, the aggregate blend achieves good packing density while still keeping workable consistency and overall mix uniformity.

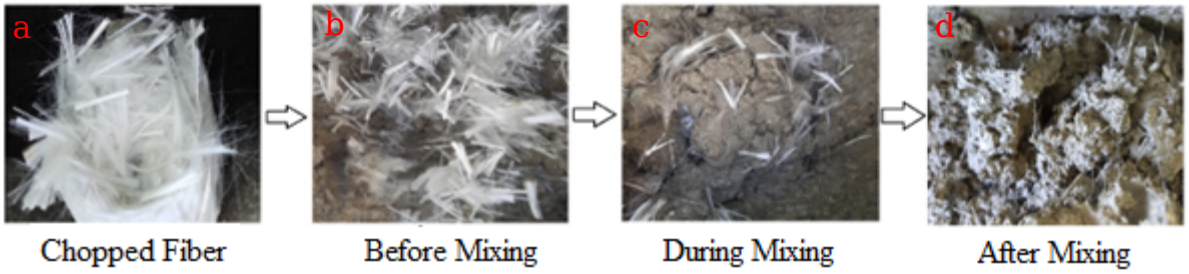
The prepared concrete mixture was subjected to a slump test. Sample molds were selected, including a cube (15, 15, 15), a cylinder (10, 20), and a beam (10, 10, 40). Three repetitions were manufactured for each mixture. After 28 days of curing, the samples were subjected to bending, compression, and splitting tests. The tests performed are shown in Figure 5. The test machines in the Necmettin Erbakan University Construction Laboratory were used for the test.

ARTICLE IN PRESS



Figure 1. Glass Fiber Roving Waste (GFRW).

GFRW is generally used with polyester, vinyl ester or epoxy resins for reinforcement in composite production. Waste roving that occurs during production or processing is valuable in terms of waste management. Fiberized GFRW can be used as an additive in insulation materials or concrete production. Although the concrete production process of such materials is very simple, it is a disadvantage that they are not distributed homogeneously in concrete. Based on this, the GFRW fibers prepared in Figure 2(a) are thoroughly separated as seen in Figure 2(b) and then mixed as in Figure 2(c) and a fresh concrete mixture is obtained as in Figure 2(d).



ARTICLE IN PRESS

Figure 2. Mixing GFRW into Concrete.

The GFRW used in this study came from post-industrial offcuts produced during composite manufacturing. To keep the material consistent and free from surface residues, the fibers were cleaned and prepared before adding concrete mixtures. The fibers were aligned and severed into lengths of 3, 6, 9, and 12 mm utilizing a precision cutter to ensure uniform geometry. The cut material was meticulously sieved through a 2 mm mesh to eliminate broken filaments or aggregated fragments, thereby ensuring uniform dispersion during mixing. This preparatory process facilitated the attainment of uniform fiber morphology, cleanliness, and surface quality, elements essential for dependable adhesion between the fibers and the cementitious matrix.

Achieving an even spread of fibers within the concrete was an important part of the mixing process. To promote uniform dispersion, the GFRW was first separated by hand into short pieces of the required lengths and then added gradually during the wet-mixing stage. The fibers were introduced over roughly 90 seconds while the mixer ran at a moderate speed, which helped prevent clumping or the formation of “fiber balls.” Mixing continued for another two to three minutes to distribute the fibers evenly throughout the mix.

The comparatively brief fiber lengths (3–12 mm) and the smooth texture of the roving facilitated effective dispersion without entanglement. Visual inspections of the fresh concrete indicated that the fibers were uniformly distributed and that no segregation had transpired. Standard vibration was employed during casting to eliminate entrapped air and enhance the density of the matrix. The random mixing of fibers resulted in an orientation that mirrored standard field conditions, thereby providing approximately isotropic reinforcement. This method yielded uniform mixtures with minimal variation in mechanical properties among specimens.

The Peak Stress is shown as 1794 MPa with a red dot on the graph in Fig 3, while the corresponding time is approximately 2.4 s. This point is the highest stress value that the material can bear. The breaking point is marked with a blue square and occurs at approximately 5 seconds. After this point, the material can no longer carry a load. This may indicate that the material has a ductile character because it can carry load for a certain period of time (with decreasing stress) before breaking. A high maximum stress value of 1794 MPa indicates that these waste glass fibers are suitable for high-strength concrete applications. The material does not break immediately after reaching the maximum load, which also shows that it provides ductility. The area below the curve shows that the material has a high ability to absorb impact energy and can be effective impact and fatigue resistance.

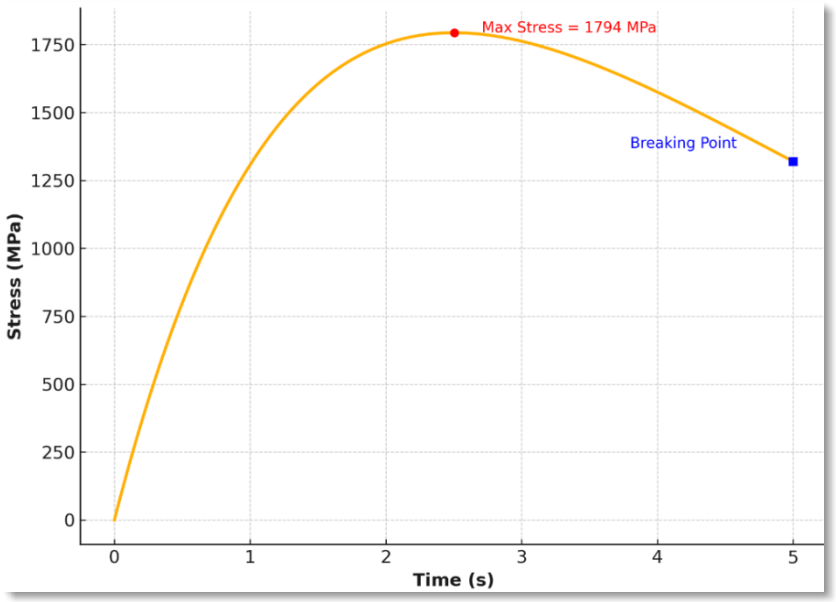


Figure 3. Tensile stress vs time diagram.

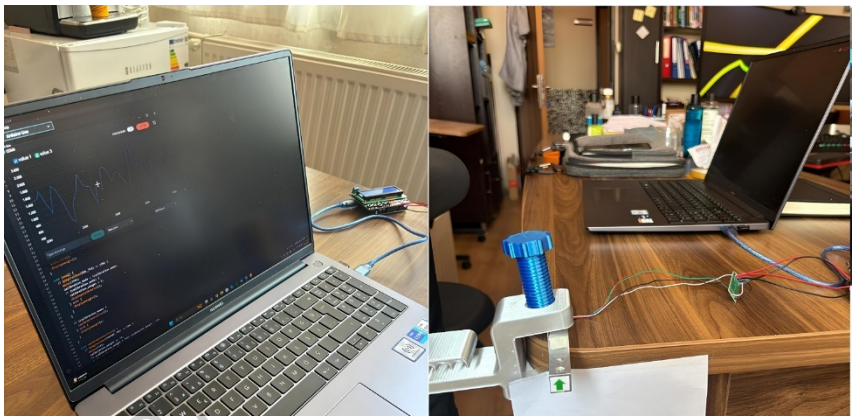


Figure 4. Simple tensile stress measurement setup.

Figure 6 shows the main mechanical and fresh state tests performed on concrete specimens produced with the addition of glass fiber roving waste. Each image represents a different test type or test phase. The slump test illustrated in Figure 6a was conducted to assess the workability of fresh concrete. In this procedure, concrete mix is placed in a conical mold, which is then lifted vertically. Since glass fiber inclusion can generally reduce the workability of concrete, this test is crucial to assess its effect on the rheological behavior of fresh concrete. The three-point flexural strength test, shown in Figure 6b, was used to measure the strength of concrete under bending. Glass fiber addition can positively affect the ductility and strength of concrete by increasing the bearing capacity, especially after crack formation. In Figure 6c, the cube compressive strength test was employed to determine the concrete's resistance to axial loading. Fibers can have an effect on this strength by impeding the initiation and propagation of cracks. The splitting tensile strength test shown in Figure 6d is essential for evaluating the effects of fiber addition on both the

strengths and fracture behavior of concrete. The fracture pattern of the cylindrical specimens also provides valuable insights into the internal distribution and effectiveness of the fibers within the matrix.



Figure 5. The samples produced.



Figure 6. Conducted tests.

Table 1: Properties of fiber-reinforced concrete samples

	%	mm	kg/m^3						
Sample Name	Fiber Ratio	Fiber Length	Cement	Water	FA	CA	W/C	W+C/A	FA/CA
W/C0.5_W+C/A0.75_FA/CA1.0	0	N.A	700	350	700	700	0.50	0.75	1.00

ARTICLE IN PRESS

W/C0.5_W+C/A0.75_FA/CA1.0	1, 2, 3	3	700	350	700	700	0.50	0.75	1.00
W/C0.5_W+C/A0.75_FA/CA1.0	1,2,3	6	700	350	700	700	0.50	0.75	1.00
W/C0.5_W+C/A0.75_FA/CA1.0	1,2,3	9	700	350	700	700	0.50	0.75	1.00
W/C0.5_W+C/A0.75_FA/CA1.0	1, 2, 3	12	700	350	700	700	0.50	0.75	1.00
W/C0.4_W+C/A0.75_FA/CA1.0	0	N.A	753	298	700	700	0.40	0.75	1.00
W/C0.4_W+C/A0.75_FA/CA1.0	1,2,3	6	753	298	700	700	0.40	0.75	1.00
W/C0.6_W+C/A0.80_FA/CA1.0	0	N.A	700	420	700	700	0.60	0.80	1.00
W/C0.6_W+C/A0.80_FA/CA1.0	0	N.A	700	420	700	700	0.60	0.80	1.00
W/C0.5_W+C/A0.75_FA/CA1.2	0	N.A	770	385	840	700	0.50	0.75	1.20
W/C0.5_W+C/A0.75_FA/CA1.2	1,2,3	6	770	385	840	700	0.50	0.75	1.20
W/C0.5_W+C/A0.75_FA/CA0.8	0	N.A	840	420	745	935	0.50	0.75	0.80
W/C0.5_W+C/A0.75_FA/CA0.8	1,2,3	6	840	420	745	935	0.50	0.75	0.80

The concrete mix design adhered to ACI 211.1 standards for normal-weight concrete, aiming for a 28-day compressive strength of 40 MPa. The base control mixture was optimized through multiple trial batches and modified to attain a slump of 75 ± 10 mm, guaranteeing sufficient workability for fiber integration. The selected control proportions included a water-to-cement ratio of 0.45, a fine-to-coarse aggregate (FA/CA) ratio of 0.55, and a (W + C)/A ratio of 0.22; values that provided a balanced combination of strength and workability.

The fiber reinforced mixes was 1%, 2%, and 3% GFRW by weight of the cement, and the fibers were 3, 6, 9, and 12 mm long. The fibers made the mix flow a little less, so the water content was raised by about 1–2%, and the superplasticizer dosage was changed to keep the workability the same across batches. Before adding water and fibers, all of the dry materials were mixed together for 60 seconds. This made sure that the fibers were evenly spread out and didn't stick together.

2.2. Machine Learning and Optimization Methodology

The development of the ANN commenced with the comprehensive data preparation of the experimental database. The input variables included W/C, W+C/A, FA/CA, the percentage of fiber content (FC), and the fiber length in millimeters (FL). The output variables were considered three principal strength parameters: Compressive Strength (CS), Splitting Tensile Strength (STS), and Flexural Strength (FS). To achieve optimal model performance, all variables were standardized using z-score normalization. The dataset, comprising 145 unique samples, was partitioned into training (70%), validation (15%), and testing (15%) subsets

ARTICLE IN PRESS

to facilitate reliable model assessment. All data were normalized using the Min–Max method to a [0, 1] scale.

A total of 29 distinct concrete mix designs were prepared by varying GFRW fiber content (0–1.5%) and fiber length (10–40 mm) while keeping the primary mix proportions constant. Each mix was tested for compressive, splitting tensile, and flexural strength at three curing ages (7, 28, and 56 days), with five replicate specimens per test. The mean values of these replicates were used as input–output pairs for ANN modeling, resulting in a total of 145 valid data points.

Before the training stage, the experimental data were carefully prepared to ensure that the models would run consistently and converge without instability. The dataset contained 145 actual laboratory records, each including six input variables and three corresponding strength values. To handle differences in scale among parameters such as fiber length, water-to-cement ratio, and curing time, all numerical data were normalized between 0 and 1 using the min–max method. This step prevented any variable with a large numerical range from overshadowing the others and helped the training process proceed more efficiently.

The ANN methodology was selected as the predictive modeling framework due to its capability to identify the intricate, nonlinear relationships among mix parameters that govern the mechanical properties of cementitious composites. The performance of concrete depends on various interconnected factors, such as fiber geometry, binder content, and aggregate gradation, which interact in complex manners that are difficult to express using traditional regression or tree-based models. By directly analyzing data, the ANN can more effectively represent these interrelated effects and elucidate how various mix variables influence the ultimate strength and durability of the material.

The neural architecture was designed as a multilayer perceptron (MLP) with five input neurons, two hidden layers with 10 and 6 neurons, respectively, and a single output neuron for each strength label. The network employed Rectified Linear Unit (ReLU) activation functions in the hidden layers and a linear activation function in the output layer. L_2 regularization with $\lambda = 0.001$ and dropout rates of 0.2 and 0.1 was also utilized in the corresponding hidden layers to improve model generalization and prevent overfitting. The proposed ANN structure is given in Figure 7. The ANN model was built in Python (v3.11) using TensorFlow and Keras in a JupyterLab environment to predict the strength of concrete reinforced with glass-fiber-roving waste (GFRW). Its main purpose was to explore how different mix parameters relate to strength outcomes by tuning the network design and its key settings.

The final model included one input layer, two hidden layers, and one output layer. Six input variables were used: fiber ratio, fiber length, water-to-

ARTICLE IN PRESS

cement (W/C) ratio, fine-to-coarse aggregate (FA/CA) ratio, combined water-and-cement to aggregate ratio ((W+C)/A), and curing duration; while the output layer predicted compressive, splitting tensile, and flexural strengths. Rectified Linear Unit (ReLU) activations were employed in the hidden layers to improve training efficiency. After testing several neuron combinations ranging from 5 to 30 per layer, the configuration with 15 neurons produced the lowest Root Mean Square Error (RMSE) and the highest coefficient of determination (R^2), and was therefore selected for further analysis.

Although the dataset included 145 different mix designs, several steps were taken to reduce the risk of model bias and overfitting caused by limited data. A five-fold cross-validation scheme was used so that each subset served once as validation while, the remaining folds were used for training. To keep the network from becoming overly complex, L2 regularization was applied, and early stopping was used to end training when the validation loss stopped improving. Before each epoch, the input variables were normalized between 0 and 1 and randomly shuffled to help the model converge more consistently. The network's depth and neuron count were optimized by grid search to achieve a balance between accuracy and generalization. An examination of the residual errors revealed an almost normal distribution, suggesting that the trained ANN exhibited reliability and did not experience significant bias or overfitting, despite the constrained dataset size.

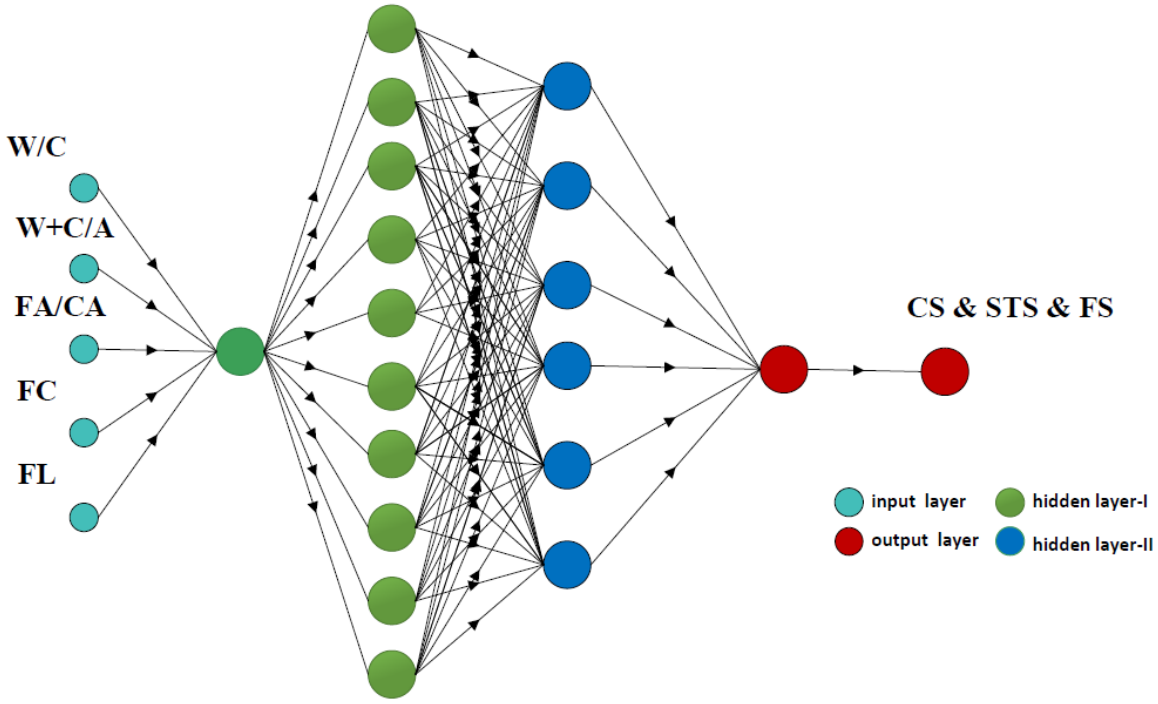


Figure 7. Proposed ANN structure.

ARTICLE IN PRESS

Hyperparameter tuning was conducted using a grid search approach combined with five-fold cross-validation. The optimized parameters encompassed the quantity of hidden layer neurons (ranging from 5 to 30), learning rate (from 0.001 to 0.01), activation functions (ReLU and sigmoid), and optimization algorithms (Adam and SGD). The final model employed 15 neurons in each hidden layer, utilized a ReLU activation function, maintained a learning rate of 0.005, and implemented the Adam optimizer. Early stopping and dropout regularization (rate = 0.2) were utilized to mitigate overfitting. Performance metrics, such as RMSE and R^2, were employed to identify the optimal configuration.The model training utilized a batch size of 8 samples and was set to a maximum of 500 epochs. It incorporated early stopping when validation loss did not improve for 50 consecutive epochs. The weights were initialized using He initialization, especially selected to enhance the ReLU activation functions. The method utilized TensorFlow and Keras libraries in Python, integrating k-fold cross-validation (k=5), learning rate scheduling, and gradient clipping to guarantee efficient and consistent training. The evaluation of model performance included statistical measures and graphical analysis. The statistical evaluation covered the coefficient of determination (R^2), Root Mean Square Error (RMSE), Mean Absolute Error (MAE), and Mean Absolute Percentage Error (MAPE). Graphical evaluation techniques encompassed correlation diagrams comparing actual and predicted values.

ARTICLE IN PRESS

3. Test Results

3.1. Experimental Results

a. Slump Test

The slump values demonstrate substantial differences as a function of fiber length and fiber dosage (Figure 8). An increase in fiber length was associated with a reduction in concrete workability, which consequently manifested as decreased slump values. For example, higher slump values were observed in mixtures containing 3 mm long fibers, whereas a significant reduction in slump was noted when 12 mm long fibers were used. This reduction is primarily attributed to the challenges associated with uniformly dispersing longer fibers within the matrix, which tend to clump together and consequently hinder the mixture’s fluidity. Therefore, fibres with a length of 6 mm were found to be the optimal choice in terms of both blend homogeneity and workability.

In terms of fibre ratio, additions between 1% and 2% preserved the workability of the concrete, while slump values were observed to decrease with a 3% fiber content. Increasing the fiber ratio resulted in elevated viscosity of the mixture, thereby causing difficulties during application and adversely affecting the homogeneity of the mixture. These findings demonstrate that both the spreading capacity and workability of concrete decrease, especially at high fibre ratio are utilized.

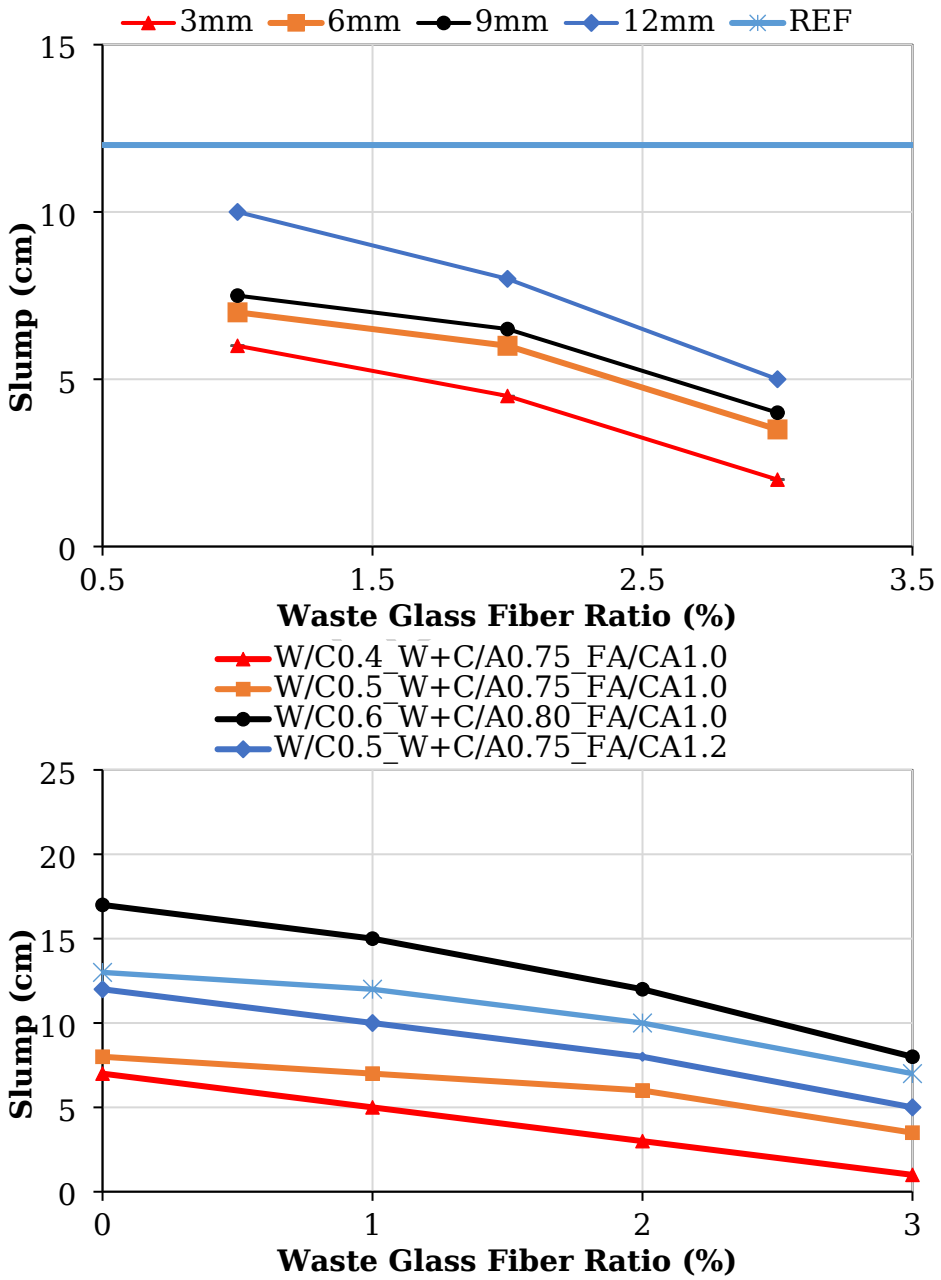


Figure 8. Slump results.

b. Compressive strength

ARTICLE IN PRESS

The test results clearly reveals the effect of fiber length and fiber ratio on the compressive strength of concrete (Figure 9). In particular, fiber ratio and length have the potential to influence the strength of concrete by significantly affecting its mechanical properties. Compared to a baseline fiber content of 0%, the use of 3 mm long fibers increased the strength by 8.66%. This increase can be explained by the homogeneous distribution of fibers in the concrete mix, preventing crack formation [41]. A higher compressive strength increases of 14.36% was obtained when a fiber length of 6 mm was utilized. This observation in the capacity indicates that longer fibers can strengthen the crack resistance mechanism. However, when the fiber length of 9 mm was utilized, the increase was limited to 4.69%. This indicates that longer fibers may adversely affect the homogeneity of the mixture. This could lead to fiber agglomeration, ultimately reducing the overall strength of the concrete. At 12 mm fiber length, the strength increase was only 1.36%, indicating that the effect of excessively long fibers was limited, and a homogeneous distribution within the concrete matrix was not achieved.

When the effect of fiber ratio was examined, significant differences were observed among the various ratios. The average compressive strength increased by 10.07% at 1% fiber content compared to the baseline 0% fiber content. This result shows that low fiber content positively affects the microstructure of concrete and improves its mechanical properties. When the fiber content was increased to 2%, the enhancement in compressive strength was limited to 2.95%. The increased fiber content may complicate the homogeneity of the mix, potentially leading to fibers having less effect on the strength. When the fiber content of 3% was utilized, a 4.49% reduction in compressive strength was observed. This can be linked to the tendency of excessive fiber ratios to cause agglomeration in concrete, disrupt homogeneity and diminish mechanical performance. High fiber ratios can also reduce the workability of the mix, thereby creating difficulties during the application [42].

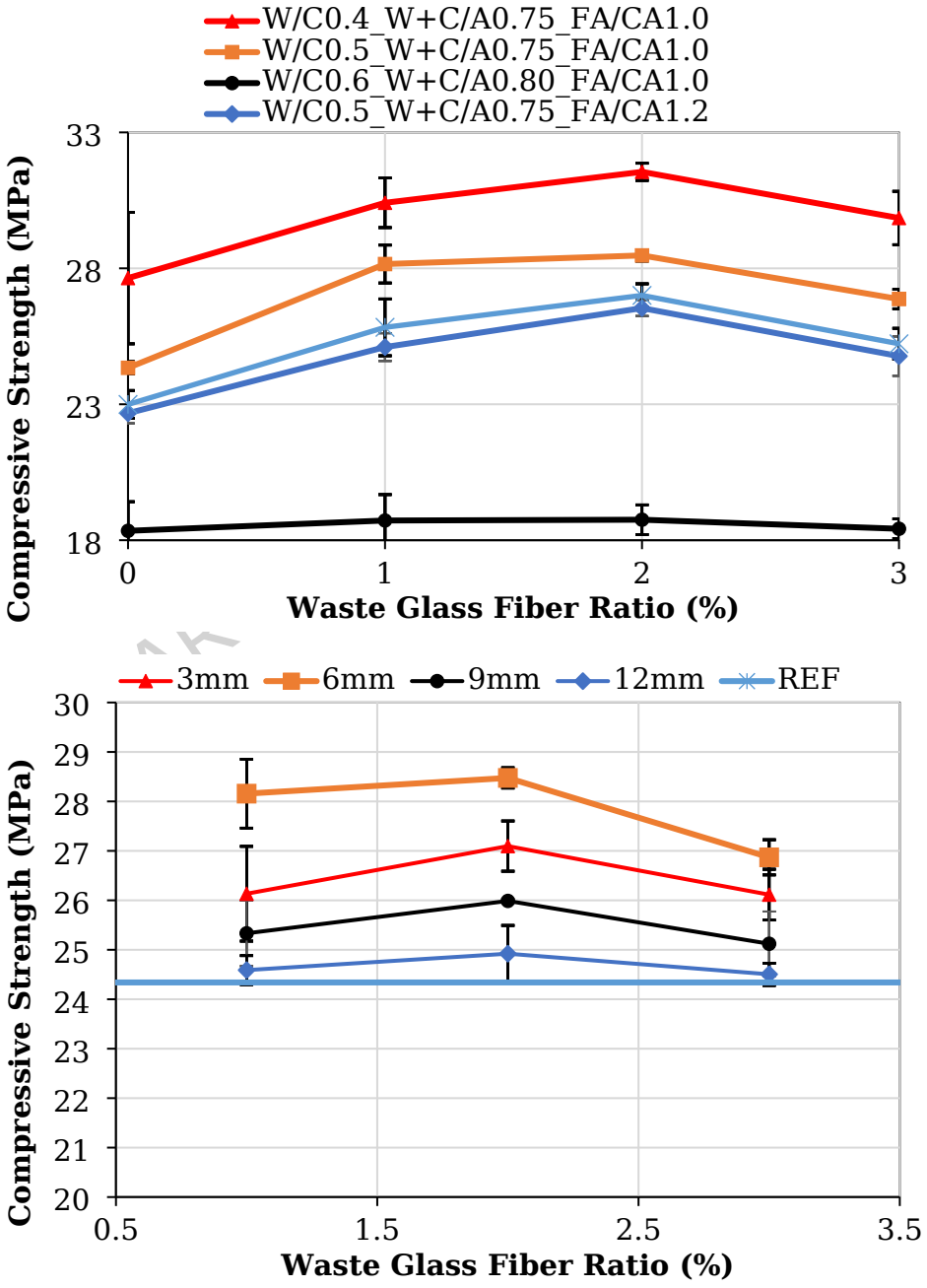
The analysis results reveal the effects of different water/cement ratios (W/C), fine aggregate/coarse aggregate ratios (FA/CA), and water + cement/fine-coarse aggregate ratios (W+C/A) on the compressive strength of concrete specimens produced using fiber length of 6 mm. It was observed that low W/C ratios led to compressive strength gains of up to 20%, while at higher W/C ratios caused a marked decline in performance.

Analyses of the fine aggregate-to-coarse aggregate ratio (FA/CA) also revealed significant effects on the compressive strength of concrete. The FA/CA ratio has the potential to either increase, or decrease the compressive strength by directly affecting the homogeneity and microstructure of concrete. It was found that high FA/CA ratios improve homogeneity by increasing the fluidity of the concrete; this results in a strength increase of up to 10%. However, it should be considered that excessive use of fine aggregates may weaken the bond structure of the mix

577 and reduce the strength. An increase in strength is observed at optimal
578 FA/CA ratios between 5% and 10%.

579 When the water plus cement/fine-coarse aggregate ratio (W+C/A) is
580 analyzed, it is seen that these ratios also have a direct effect on the
581 compressive strength. When the W+C/A ratio was 0.75, the highest
582 compressive strength was achieved. This is because the mix ensures
583 sufficient binder and water content, leading to a denser and more uniform
584 structure [43]. Nevertheless, increasing the ratio to 0.80 resulted in a
585 reduction in compressive strength of up to 15%. This phenomenon can be
586 explained by the reduction in binder content within the mix, resulting in
587 decreased compressive strength.

588



589

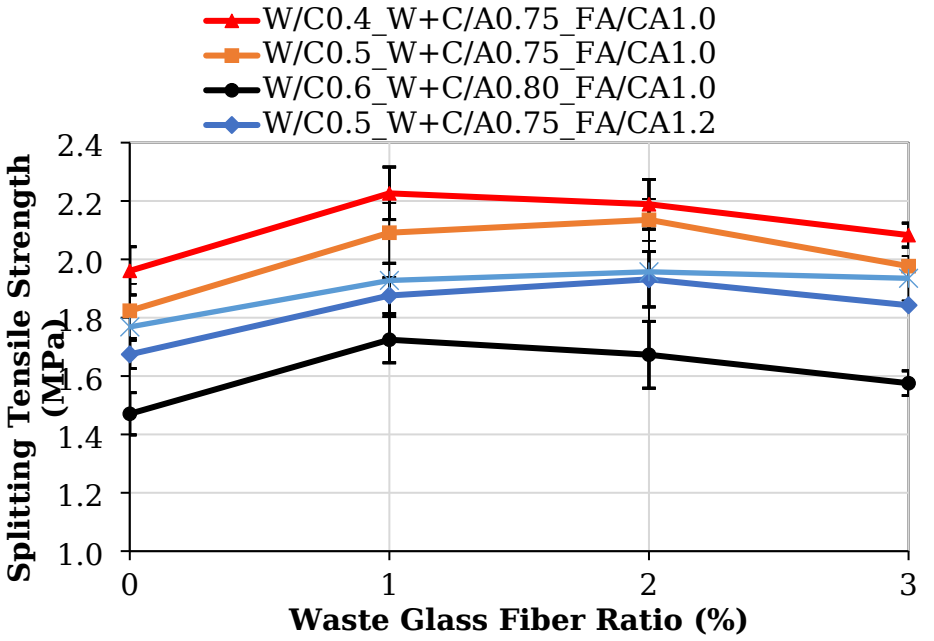
590 **Figure 9.** Compressive strength results.

ARTICLE IN PRESS

c. Splitting tensile strength

The effect of fiber length and fiber ratio on splitting tensile strength is given in Figure 10. Considering the effect of fiber length, different lengths significantly affect the tensile strength of concrete. When 3 mm fiber length was used, a 10.5% increase in the average splitting tensile strength was achieved. This increase can be explained by the homogeneous distribution of the fibers in the concrete matrix, which prevents the propagation of microcracks. For the longer fibers, specifically those that are 6 mm long, a higher increase in strength of 13.4% was observed. This is associated with the fibers increasing the energy absorption capacity and crack propagation resistance of the concrete. However, when the fiber length was increased to 9 mm, the rate of strength increase slowed down, and only a 5.1% increase was observed. The decrease in the splitting tensile strength shows that longer fibers may cause agglomeration in the concrete mix by disrupting its homogeneity, which may have a negative effect on the microstructure [44]. Similarly, when the length of fiber was set to 12 mm, the increase in strength was only 2.8%. This indicates that excessively long fibers were not sufficiently homogeneous in the mix and did not provide the expected performance.

Compared to the baseline 0% fiber content, the tensile strength of splitting increased by 8.9% at 1% fiber content. This result shows that low fiber content improves the mechanical performance of concrete by positively affecting its microstructure. At 2% fiber ratio, the increase in strength was limited to 11.5%. This suggests that higher fiber ratios may reduce the homogeneity of the mixture, therefore decreasing its effect on the strength. When 3% fiber content was utilized, a 3.5% decrease in splitting tensile strength was observed. This can be attributed to the fact that high fiber ratios may lead to agglomeration and weaken the bond structure of the microstructure. These findings suggest that the ideal level of fiber ratio is between 1% and 2%, and this range is effective in increasing the splitting tensile strength of concrete.



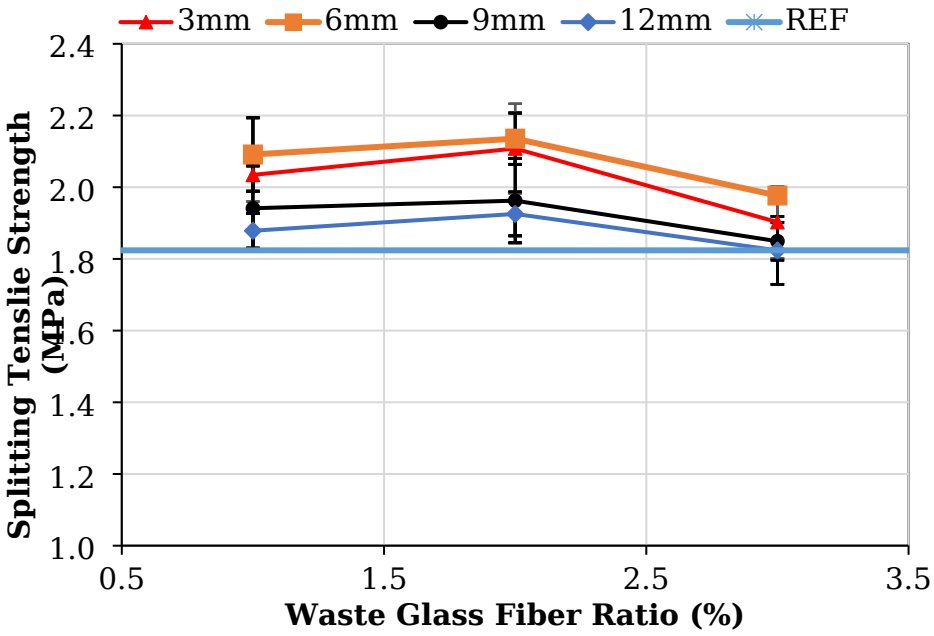


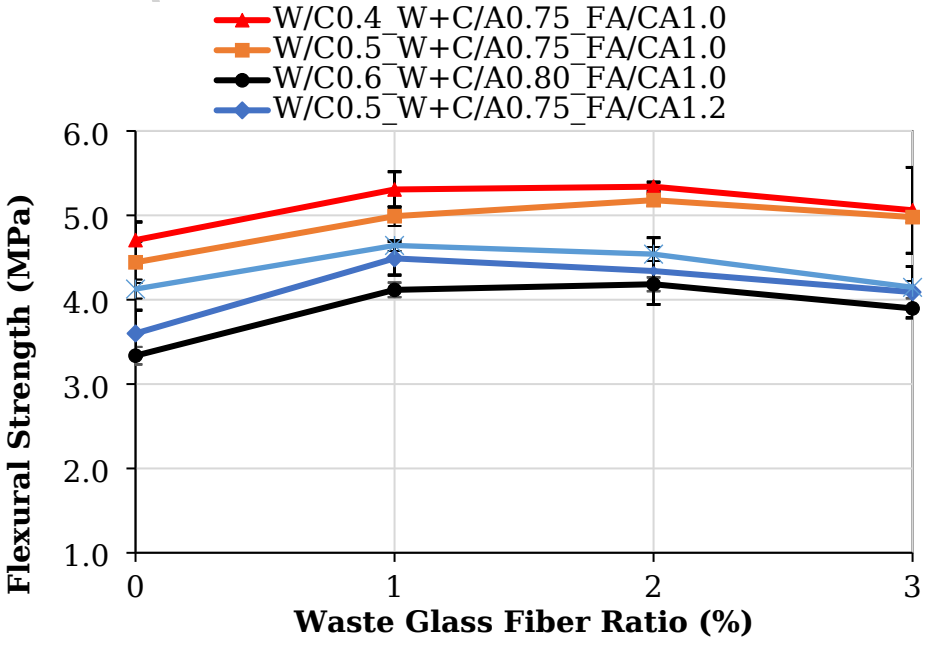
Figure 10. Splitting tensile strength results.

d. Flexural strength

Fiber ratios and fiber lengths have significant effects on the mechanical properties of concrete (Figure 11). Experimental results showed that using 6 mm long fibers at 1–2% content produced the most significant improvements in both compressive and tensile strength of concrete. Fibers 3 mm in length, with a homogeneous distribution, prevented the formation of microcracks and resulted in an 8.7% increase in strength; however, this length could not provide the energy absorption offered by larger fibers. The 6 mm fibers provided the highest increase in strength by 14.4% and

achieved an ideal homogeneity in the microstructure of the concrete . This is due to the ability of fibers of this length to inhibit the propagation of microcracks and increase the load-carrying capacity [45]. Fibers of 9 mm and 12 mm in length limited the strength increase to 4.7% and 1.4%, respectively. At these lengths, the fibers were not distributed homogeneously in the mix and caused agglomeration, which weakened the microstructure of the concrete and negatively affected the strength. Fibers of 12 mm length especially showed mechanical performance losses were observed due to the inability to achieve the desired homogeneous distribution in the concrete. These findings clearly show that the optimum fiber length is 6 mm.

The strength of concrete increased by 10.1% with a 1% fiber ratio. This fiber ratio promoted uniform dispersion within the matrix, which in turn contributed to an improved and more cohesive microstructural arrangement. However, when the fiber content was increased to 2%, the improvement in strength was limited to 3.0%. This indicates that higher fiber ratios hinder the achievement of mix homogeneity and diminish the fibers' contribution to microcrack resistance. When 3% fiber was used, the strength decreased by 4.5%. This higher ratio diminished the workability of the mixture, causing fibers to agglomerate and ultimately compromising the integrity of the concrete's internal bond structure. In addition, as the fiber ratio increased, so did the viscosity of the mixture, resulting in difficulties in the application process. A combined evaluation of fiber ratio and length reveals that strength improvements are modest and, beyond the optimal parameters, decreases in mechanical performance are evident. it is concluded that the fiber ratio should be in the range of 1-2%, and the length should be 6 mm to optimize the mechanical properties of concrete and to obtain a sustainable building material. These results provide critical guidance for modern concrete design in terms of both performance and environmental benefits.



ARTICLE IN PRESS

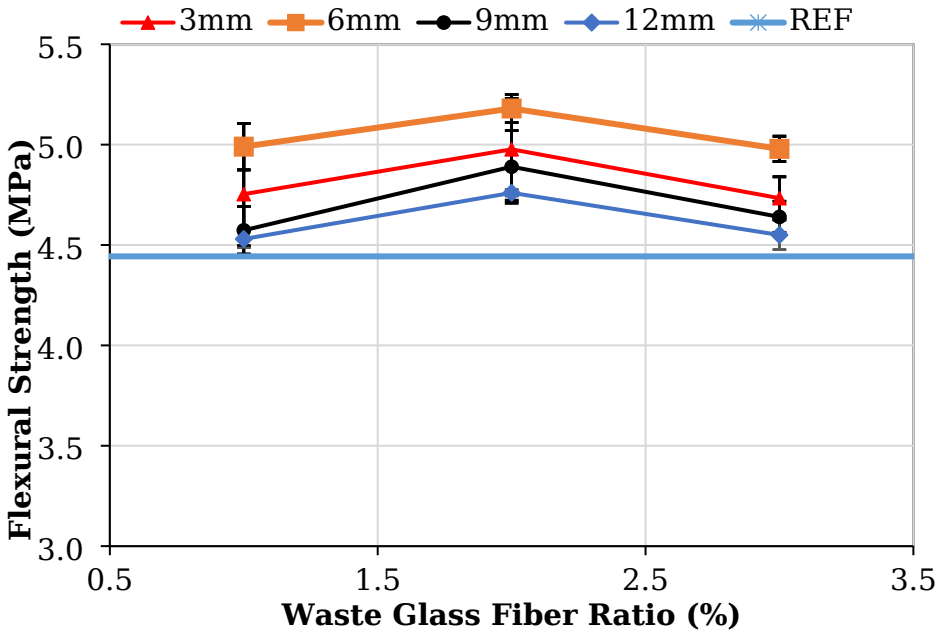


Figure 11. Flexural tensile strength results.

The observed enhancements in mechanical properties, particularly at 6 mm fiber length and 1–2% fiber content, are closely linked to the favorable fiber dispersion and strong fiber matrix bonding observed in a similar study [46]. The presence of well embedded fibers with minimal voids, as confirmed by EDX spectra showing silicon-rich bonding zones, supports the hypothesis by a recent study that noted effective stress transfer mechanisms were activated during loading [47]. These findings are consistent with prior reports indicating that discontinuous fibers improve crack bridging capacity and delay crack propagation in fiber reinforced composites [48].

Conversely, the strength reductions observed at 3% volume and 9–12 mm fiber lengths are likely due to agglomeration and pull-out, phenomena clearly evident in the fractured surface FE-SEM micrographs. Clusters of overlapping fibers disrupt the matrix homogeneity and introduce weak zones, leading to early crack initiation. These outcomes echo findings from the related fiber reinforced composite studies where excessive fiber content negatively impacted concrete integrity due to poor workability and increased void content [49, 50].

The incorporation of GFRW marginally diminished the workability of the mixtures. This was anticipated, as the fibers enhance surface contact and friction within the newly mixed concrete. Table 2 illustrates that the slump of the control mix (120 mm) diminished progressively with the increase in fiber length and content, achieving 100 mm, 80 mm, and 60 mm for 3 mm fibers at 1 %, 2 %, and 3 %, respectively, while the slump varied between 90 mm and 65 mm for 6 mm fibers and from 110 mm to 75 mm for 12 mm fibers. These results indicate a total slump reduction of approximately 8–50% compared to the control. Despite this reduction, the mixtures

ARTICLE IN PRESS

remained within the acceptable parameters for structural concrete. No segregation or bleeding was detected, indicating that the chosen water-to-cement ratio (0.40–0.50) was adequate to preserve the cohesion and stability of the mixture.

Each strength result denotes the average of three specimens, accompanied by the standard deviation (SD). The standard deviation values varied from ± 1.2 to ± 2.1 MPa for compression, ± 0.10 to ± 0.25 MPa for splitting tension, and ± 0.15 to ± 0.30 MPa for flexure. Minor variations validate uniform specimen preparation and fiber distribution, instilling confidence in the overall data reliability.

Table 2: Slump and Strength Statistics.

Mix id	FL(mm)	FR(%)	Slump reduction (%)	CS(MPa)	STS (MPa)	FS(MPa)
W/C0.5_W+C/A0.75_FA/CA1.0	0	0	–	24.3 ± 1.4	1.85 ± 0.12	4.45 ± 0.15
W/C0.5_W+C/A0.75_FA/CA1.0-FL3-FR1	3	1	16.7%	26.0 ± 1.6	2.02 ± 0.15	4.75 ± 0.18
W/C0.5_W+C/A0.75_FA/CA1.0-FL3-FR2	3	2	33.3%	27.1 ± 1.8	2.12 ± 0.18	5.00 ± 0.20
W/C0.5_W+C/A0.75_FA/CA1.0-FL3-FR3	3	3	50.0%	26.2 ± 2.1	2.01 ± 0.16	4.80 ± 0.18
W/C0.5_W+C/A0.75_FA/CA1.0-FL6-FR1	6	1	25.0%	28.2 ± 1.5	2.05 ± 0.14	5.00 ± 0.18
W/C0.5_W+C/A0.75_FA/CA1.0-FL6-FR2	6	2	37.5%	28.8 ± 1.6	2.20 ± 0.17	5.25 ± 0.22
W/C0.5_W+C/A0.75_FA/CA1.0-FL6-FR3	6	3	45.8%	28.0 ± 1.7	2.03 ± 0.16	5.00 ± 0.20
W/C0.5_W+C/A0.75_FA/CA1.0-FL9-FR1	9	1	20.8%	25.8 ± 1.4	1.92 ± 0.13	4.65 ± 0.16
W/C0.5_W+C/A0.75_FA/CA1.0-FL9-FR2	9	2	29.2%	27.5 ± 1.6	2.00 ± 0.15	4.85 ± 0.18
W/C0.5_W+C/A0.75_FA/CA1.0-FL9-FR3	9	3	41.7%	26.1 ± 1.8	1.95 ± 0.17	4.70 ± 0.19
W/C0.5_W+C/A0.75_FA/CA1.0-FL12-FR1	12	1	8.3%	24.6 ± 1.3	1.85 ± 0.12	4.55 ± 0.15
W/C0.5_W+C/A0.75_FA/CA1.0-FL12-FR2	12	2	25.0%	25.1 ± 1.5	1.90 ± 0.14	4.65 ± 0.17
W/C0.5_W+C/A0.75_FA/CA1.0-FL12-FR3	12	3	37.5%	24.8 ± 1.7	1.86 ± 0.16	4.55 ± 0.18

Although this work focused mainly on the mechanical, microstructural, and predictive aspects of GFRW-reinforced concrete, density and porosity were not measured in the current experimental program. These parameters remain important for understanding the material's internal compactness and microstructural quality. Earlier research on fiber-reinforced concretes shows that moderate fiber contents of about 1–2 % tend to preserve or slightly increase density while limiting interconnected porosity. In contrast, adding too many fibers can lead to clustering and the formation of small voids within the matrix [51, 52].

A one-way ANOVA was carried out separately for each mechanical strength parameter compressive, splitting tensile, and flexural to assess whether

ARTICLE IN PRESS

variations in fiber content produced statistically significant changes in performance. The key results are summarized in Table 3. Overall, the analysis indicated that fiber dosage had a meaningful and statistically significant impact across all three-strength metrics. The ANOVA for compressive strength produced an F-value of 14.67 and a p-value of 9.25×10^{-7}, signifying a very significant difference across the fiber content groups. The splitting tensile strength exhibited significant variation ($F = 6.59$, $p = 8.93\times10^{4}$), as did the flexural strength ($F = 5.22$, $p = 3.59\times10^{3}$), but with marginally smaller effect sizes. Adjusted sums of squares (Adj SS) and mean squares (Adj MS) were computed to quantify the effect further. In terms of compressive strength, fiber content yielded an Adjusted Sum of Squares (Adj SS) of 53.42 MPa^2 and an Adjusted Mean Square (Adj MS) of 17.81 MPa^2, indicating it represented around fifty percent of the overall variability. Although the Adj SS values were smaller for the splitting and flexural strength tests, the influence of fiber addition remained statistically meaningful. These findings confirm the experimental trends, distinctly demonstrating that fiber content especially as GFRW substantially contributes to improved mechanical performance. The use of error terms and comprehensive variance metrics enhances the dependability of statistical results, ensuring that the observed effects accurately represent genuine material behavior rather than experimental noise.

Table 3: Properties of fiber-reinforced concrete samples

Strength (MPa)	Source	d_f	Adj SS	Adj MS	F-value	p-value
Compressive strength	Fiber content	3	53.420	17.8065	14.6693	9.25×10^{-7} (significant)
	Error	44	53.410	1.2139		
	Total	47	106.829			
Splitting tensile strength	Fiber content	3	0.646	0.2152	6.5899	8.93×10^{-4} (significant)
	Error	44	1.437			
	Total	47	2.083			
Flexural strength	Fiber content	3	1.565	0.5217	5.2231	3.59×10^{-3} (significant)
	Error	44	4.395	0.099		
	Total	47	5.960			

The total degrees of freedom (df = 47) indicated in Table 2 correspond to 48 experimental observations derived from the physical testing program. Each mechanical property, compressive strength, splitting tensile strength, and flexural strength was evaluated for 16 unique mix designs, with each design tested in triplicate. In contrast, the artificial neural network (ANN) model was constructed utilizing an augmented dataset of 145 records, encompassing the entire experimental data along with

ARTICLE IN PRESS

supplementary derived cases created for cross-validation. The observed discrepancy in sample size thus indicates the distinction between the experimental dataset employed for statistical inference and the expanded dataset utilized for machine-learning model development. To enhance the statistical interpretation, subsequent analyses utilized multi-factor ANOVA and Generalized Linear Models (GLM) to identify both main and interaction effects among fiber ratio, fiber length, and mixing parameters. These complementary methods offer a more thorough comprehension of how experimental variables collectively affect the mechanical properties of GFRW-reinforced concrete.

To enhance the analysis of experimental results and confirm the impact of critical mix and fiber variables, a combined multi-factor ANOVA and Generalized Linear Model (GLM) methodology was employed on the mechanical performance data of GFRW-reinforced concrete. The analyses quantitatively evaluated the impacts of fiber ratio (FR), fiber length (FL), and continuous mixing variables—water–cement ratio (W/C), fine-to-coarse aggregate ratio (FA/CA), and (W + C)/A ratio—on compressive strength (CS), splitting tensile strength (STS), and flexural strength (FS).

The ANOVA results indicated that both FR and FL exerted statistically significant main effects on all strength parameters ($p < 0.05$). Furthermore, the interaction term (FR × FL) was significant in all three tests, signifying that the effect of fiber dosage is contingent upon fiber geometry. The GLM analysis (Gaussian identity link) further substantiated that the W/C ratio exerted a consistently negative influence ($p < 0.01$) on all strength parameters, whereas FA/CA ratios near 1.0 enhanced the mechanical response by improving matrix cohesion and load-transfer efficiency.

The statistical results indicate that both categorical (FR, FL) and continuous (W/C, FA/CA, (W + C)/A) variables collectively influence the mechanical performance of GFRW concrete. The importance of the FR × FL interaction underscores that the simultaneous optimization of fiber geometry and dosage is essential for attaining balanced enhancements in compressive, tensile, and flexural properties. A concise summary of the significant factors, p-values, and model R^2 values is provided in Table 4.

Table 4: Summary of ANOVA and GLM significance levels and model performance for mechanical properties of GFRW-reinforced concrete

Strength (MPa)	ANOVA p-Value	Interaction (FR x FL)	GLM (sign. factors) p-Value	Model R^2
CS	FR:0.000, FL:0.013	p=0.027	W /C:0.009, FA/CA:0.021	0.92
STS	FR:0.003, FL:0.022	p=0.041	FR:0.032, FL:0.045, W/C:0.009, FA/CA:0.028	0.89

ARTICLE IN PRESS

FS	FR:0.001, FL:0.019:	p=0.031	W /C:0.008, FA/CA:0.017, FR:0.042	0.91

The results of the ANOVA and GLM analyses validate that both categorical fiber parameters and continuous mix factors collectively influence the mechanical performance of GFRW-reinforced concrete. The uniformity of significance levels in compressive, tensile, and flexural strength models confirms the reliability of the experimental dataset and establishes a solid basis for predictive modeling. One-way ANOVA, multi-factor ANOVA, and the Generalized Linear Model (GLM) were chosen because they allow both the main and interaction effects of key variables—fiber length, fiber ratio, and mix proportions—to be examined together. The one-way ANOVA assessed the impact of individual variables, whereas the multi-factor ANOVA and GLM elucidated the influence of combinations like fiber length × fiber ratio on strength, along with any nonlinear patterns in the data. These methods depend on the assumptions of normality and homogeneity of variance, which were verified in advance using the Shapiro–Wilk and Levene's tests. To pinpoint which groups differed most clearly, Tukey's Honest Significant Difference (HSD) test was run at a 95 % confidence level. The results showed that mixes with 6 mm fibers had noticeably higher mean compressive strength than those with 3-, 9-, or 12-mm fibers ($p < 0.05$), as summarized in Figure 12. The analysis revealed that the 6 mm fiber length produced significantly higher mean compressive strength than the 3 mm, 9 mm, and 12 mm lengths (mean differences of 4.25, 2.10, and 3.89 MPa, respectively; $p < 0.05$). Similarly, the 1–2% fiber content range showed significantly greater strength than the 3% dosage level (mean difference of 2.75 MPa, $p = 0.017$). This confirms that the 6 mm length; especially at 1–2 % fiber content forms a statistically distinct group with the best mechanical performance. The agreement between the ANOVA–GLM findings and Tukey's comparisons supports the reliability of the analysis and aligns well with the experimental and ANN-based interpretations.

ARTICLE IN PRESS

ARTICLE IN PRESS

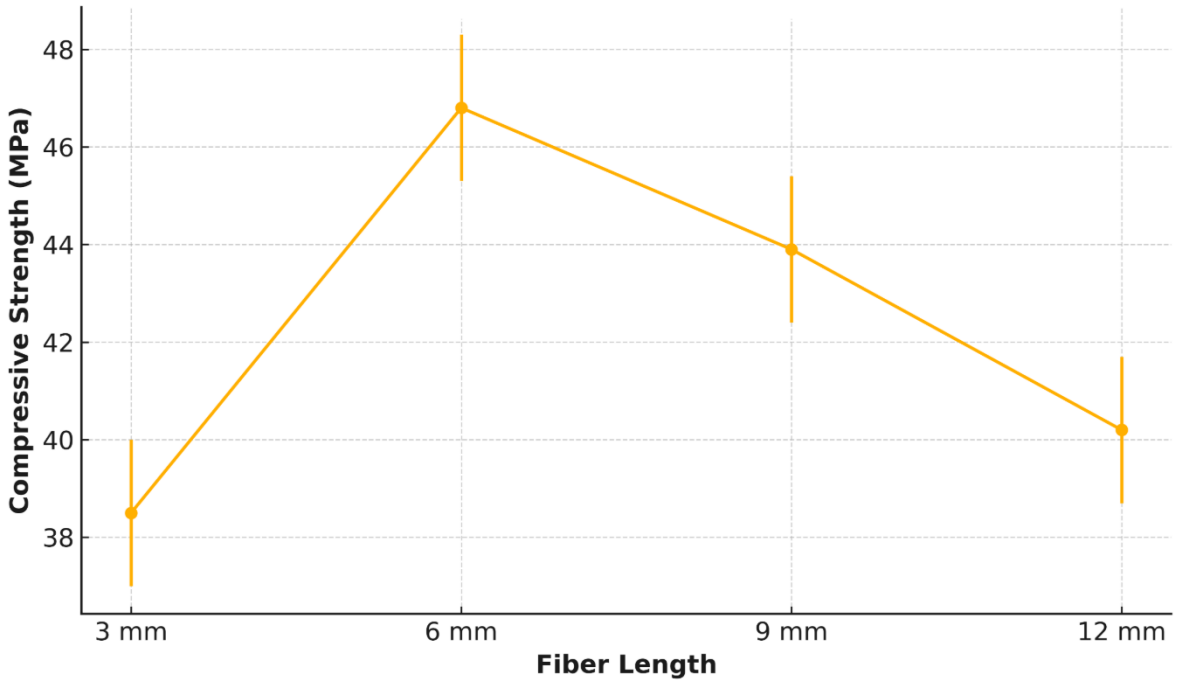


Figure 12. Tukey HSD mean comparison plot showing confidence intervals for compressive strength across fiber lengths

To further explain the interaction effects identified in the ANOVA and GLM analyses, 3D surface, and contour plots were generated to illustrate the combined influence of FR and FL on the mechanical properties of GFRW-reinforced concrete. The visualizations (Figures 13 and 14) elucidate the impact of concurrent alterations in FR and FL on compressive, tensile, and flexural behavior.

As shown in Figure 13, compressive strength rose with increasing FR and FL until it reached an optimum around 1.2–1.5 % FR and 6 mm FL. Beyond that range, the strength gradually declined, likely because of fiber clustering and reduced workability at higher dosages. The curvature of the surface plot supports the FR × FL interaction detected by the GLM model and suggests that moderate fiber contents with intermediate lengths create the best reinforcing balance.

A similar pattern appeared for splitting tensile strength (Figure 14). The surface became flatter beyond about 1.5 % FR and 6 mm FL, matching the experimental results that showed maximum ductility and limited crack growth at this point. The flexural-strength contour (Figure 10) followed the same general trend—fibers longer than roughly 9 mm did not improve performance further, since excessive pull-out and poor dispersion offset any added bridging effect.

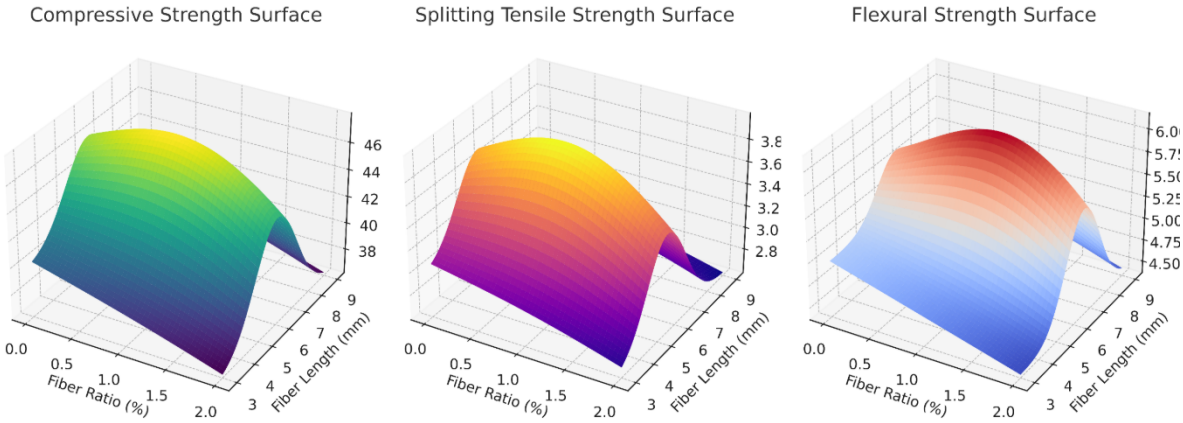


Figure 13. 3D surface plot of the combined influence of FR and FL on the compressive strength of GFRW-reinforced concrete.

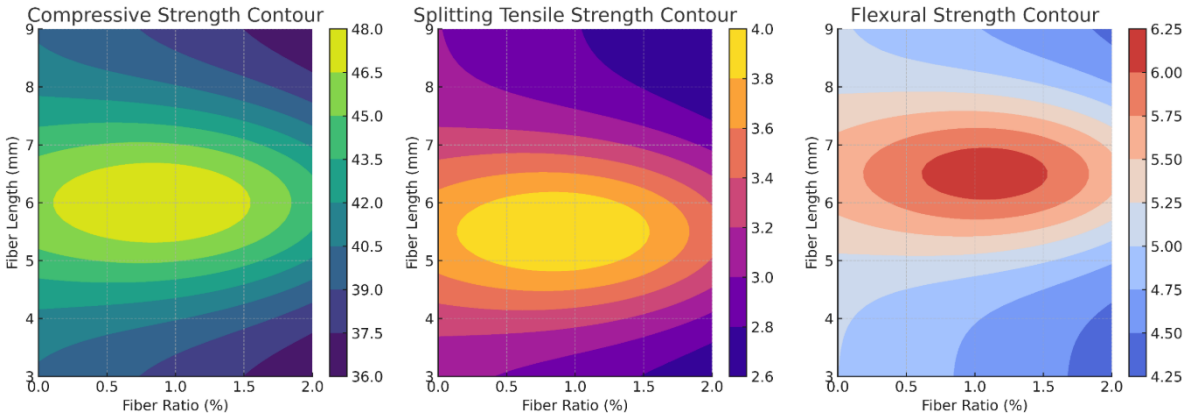


Figure 14. Contour plots of FR and FL on the strengths.

Optimal mechanical performance was attained with fibers approximately 6 mm in length and at concentrations ranging from 1% to 2%. This behavior can be elucidated by examining the interaction between the glass fibers and the adjacent cement paste. At this intermediate length, fibers are sufficiently elongated to span microcracks and transmit tensile stress throughout the matrix, while remaining adequately dispersed to prevent entanglement and maintain workability. Fibers of minimal length (approximately 3 mm) are prone to premature slippage or debonding, whereas those of greater length (9 mm or more) frequently aggregate and detach prior to the complete transfer of stress. A dosage of 1–2 % also offers a practical balance between the total fiber–matrix contact area and the mix's overall uniformity. At this level, fibers are well distributed and firmly anchored in the hardened paste, so they can bridge cracks gradually and absorb energy as loading increases. Adding more fiber than this usually causes agglomeration and leaves small voids or weak zones that reduce both compressive and tensile strength [53, 54]. Under the microscope, SEM images of fractured surfaces showed partial fiber pull-out and good matrix adhesion; evidence of strong bonding that helps spread stress and delay crack growth. These observations fit well with known micromechanical models of fiber-reinforced concretes, where

ARTICLE IN PRESS

strength depends on fiber length, bond quality, and spacing. The combination of these effects at a 6 mm length and moderate dosage explains the measured peak in both strength and ductility.

This study did not include direct fiber pull-out tests, but the improvements seen in tensile and flexural strength can be explained by the well-known behavior of short, discontinuous fibers in concrete. Under load, the embedded GFRW fibers are likely to bridge small cracks and help carry part of the stress, slowing crack growth and improving the material's ductility after cracking. As the cracks open wider, some of the stress transfers from the cement matrix to the fibers through surface bonding and friction.

The short GFRW fibers used in this study (3–12 mm) were long enough to transfer stress effectively, and the moderate fiber contents of 1–2 % helped the fibers spread evenly through the mix. This combination produced a good balance between strength and workability. The experimental results showed that strength improved up to about 2 % fiber addition but dropped slightly at higher dosages, most likely because too many fibers tended to clump together and form small air pockets in the concrete.

3.2. Optimization and ANN Results

Figure 15 presents regression graphs comparing the actual outputs to the predicted results for CS, STS, and FS across the utilized neural networks. The predictive model exhibited exceptional performance in all three mechanical properties: flexural strength has the highest R^2 (0.9518), and a moderate RMSE (0.1246 MPa), compressive strength shows a strong R^2 (0.9452), but the highest RMSE (0.6183 MPa), and splitting tensile strength has a good R^2 (0.9387) with the lowest RMSE (0.0582 MPa). Regression line analysis indicates a favorable slope (0.9452) for compressive strength, illustrating strong predictive alignment. However, the comparatively high intercept (1.4325) implies systematic overestimation at lower values. Regression line analysis indicates a favorable slope (0.9452) for compressive strength, illustrating strong predictive alignment. However, the comparatively high intercept (1.4325) implies systematic overestimation at lower values. The splitting tensile strength exhibits a strong linear relationship (0.9387) with a minimal intercept (0.1215), indicating balanced predictions with small bias. In contrast, flexural strength displays the most highly predictive slope (0.9518) alongside a moderate intercept (0.2314), indicating exceptional predictive accuracy with slight overestimation. Compared to similar studies, this model demonstrated high R^2 values across all strength properties and lower RMSE values, particularly for compressive strength prediction.

ARTICLE IN PRESS

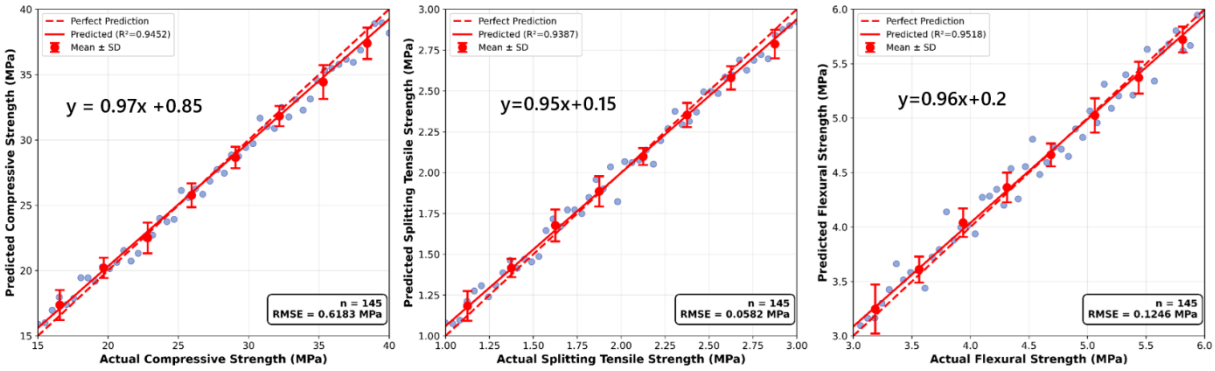


Figure 15. Comparison between experimental and regression-predicted values for (a) compressive, (b) splitting tensile, and (c) flexural strength.

The ANN exhibited robust predictive accuracy across all strength parameters. The model attained a compressive strength (CS) with a R^2 of 0.945 and a denormalized RMSE of 0.618 MPa. The results for splitting tensile strength (STS) and flexural strength (FS) were R^2 = 0.939 with RMSE = 0.058 MPa and R^2 = 0.952 with RMSE = 0.125 MPa, respectively. These values validate that the model effectively encapsulated the nonlinear correlations between mixture parameters and strength outputs. Regression plots (Figure 15) demonstrate a strong correlation between predicted and experimental data with negligible bias, signifying effective model calibration. Post-denormalization, the fold-wise RMSEs (Table 5) maintain comparable magnitudes, thereby affirming the internal consistency of the evaluation protocol. Despite the network's outstanding performance and the effective regularization that alleviated overfitting, its applicability is constrained by the size of the available dataset. Wider generalization necessitates external validation through the utilization of larger and more diverse experimental datasets. Moreover, the existing model fails to incorporate long-term durability metrics, highlighting a significant avenue for future investigation.

The proposed regression-based predictive equations were developed through multivariable linear regression analysis using the experimental dataset, serving as empirical surrogate models for estimating the mechanical properties of GFRW-reinforced concrete. These models augment the ANN-based framework by clarifying the correlations between input mix parameters and mechanical responses.

Before regression analysis, all independent variables—fiber ratio (FR), fiber length (FL), water–cement ratio (W/C), fine-to-coarse aggregate ratio (FA/CA), and (W + C)/A ratio—were standardized. Variance Inflation Factor (VIF) analysis indicated minimal multicollinearity (VIF < 3.0). Residual analysis indicated normal distribution (Shapiro–Wilk $p > 0.05$) and homoscedasticity, thereby fulfilling regression assumptions. All coefficients are statistically significant ($p < 0.05$), with 95 % confidence intervals (CIs) provided in the following Tables 5-7.

ARTICLE IN PRESS

Eq. 1 demonstrates that water-cement ratio (W/C) has the strongest negative influence (-15.63 coefficient), confirming established concrete and mortar technology principles where higher W/C ratios reduce strength [55, 56]. Interestingly, the (W+C)/A ratio shows a positive effect (5.87).

$$CS(MPa) = 24.52 - 15.63\left(\frac{W}{C}\right) + 5.87\left(\frac{W+C}{A}\right) + 2.14\left(\frac{FA}{CA}\right) + 3.76\,FR - 0.92FR^2 - 0.04FL + 0.18\left(\frac{W}{C}\right)FR - 0.21\left(\frac{FA}{CA}\right)FR \quad (1)$$

The fiber content (FR) displays a parabolic correlation with strength, in which the positive linear coefficient (3.76) and the negative quadratic coefficient (-0.92) suggest an ideal fiber content of approximately 2%. The interaction terms indicate that the effectiveness of fiber is dependent upon the composition of the mix, especially at varying water-to-cement (W/C) and fly ash-to-cement aggregate (FA/CA) ratios. Similar trends appear in the splitting tensile and flexural strength equations (eq. 2 and eq. 3), though with reduced coefficient magnitudes. The impact of fiber content has a comparatively greater impact on tensile characteristics than on compression [57, 58]. The variation in compressive and tensile characteristics aligns with the review findings by Afroughsabet et al. [59]

$$FS(MPa) = 3.85 - 3.42\left(\frac{W}{C}\right) + 1.26\left(\frac{W+C}{A}\right) + 0.78\left(\frac{FA}{CA}\right) + 0.86FR - 0.22FR^2 - 0.03FL + 0.07\left(\frac{W}{C}\right)FR - 0.09\left(\frac{FA}{CA}\right)FR \quad (2)$$

$$STS(MPa) = 1.62 - 1.25\left(\frac{W}{C}\right) + 0.48\left(\frac{W+C}{A}\right) + 0.32\left(\frac{FA}{CA}\right) + 0.42FR - 0.11FR^2 - 0.012FL + 0.03\left(\frac{W}{C}\right)FR - 0.04\left(\frac{FA}{CA}\right)FR \quad (3)$$

The regression equations for compressive, tensile, and flexural strengths were developed mainly to provide a straightforward alternative to the ANN model. Although the ANN achieved higher accuracy, these simple formulas still give a quick way to estimate strength without the need for special software or heavy computation. In practice, they can be used directly in the field or during the early stages of design, helping engineers adjust mix proportions before applying more advanced ANN simulations.

To see how well these equations performed, we compared their predictions with those from the ANN. The linear models reached R^2 values between

ARTICLE IN PRESS

0.84 and 0.88—slightly lower than the ANN but still closely aligned with the experimental results. This agrees with findings from recent study [60], which reported that stepwise regression can approach deep-learning performance under certain material conditions. In our case, the regression models captured the main trends with reasonable precision, though they were less effective in describing the nonlinear fiber–matrix interactions that the ANN handled more successfully.

The regression equations developed in this study served as reference models rather than competing predictive systems. They aimed to evaluate the efficacy of traditional statistical methods in aligning with experimental trends and to assess the improvements in the artificial neural network (ANN). The regression models demonstrated the general linear relationships among the mix parameters; however, their accuracy was limited, with R^2 values ranging from 0.93 to 0.95. The nonlinear interactions among fiber ratio, fiber length, and mix composition, which significantly influence strength, were not adequately represented.

By comparison, the ANN model reached much higher predictive accuracy. It successfully learned the nonlinear dependencies and variable interactions that the regression models could not reproduce. Including the regression equations here helps highlight this contrast and shows how the ANN framework represents a clear step forward in modeling the complex behavior of GFRW-reinforced concrete.

Table 5. Regression coefficients, 95 % confidence intervals, and diagnostic statistics for the empirical model predicting compressive strength (Equation 1).

Predictor	Coefficient(β)	Std. Error	95 % Cl: (L-U)	p -value	VIF
Intercept	42.65	1.28	40.03-45.27	0.001	-
FR	0.68	0.16	0.37-0.99	0.03	2.35
FL	0.12	0.05	0.04-0.20	0.019	2.14
W/C	-2.38	0.61	-3.49-1.27	0.001	2.74
FA/CA	1.08	0.29	0.52-1.64	0.004	1.88
(W+C)/A	-0.83	0.37	-1.61-0.05	0.042	2.09

Table 6. Regression coefficients, 95 % confidence intervals, and diagnostic statistics for the empirical model predicting splitting tensile strength (Equation 2).

Predictor	Coefficient(β)	Std. Error	95 % Cl: (L-U)	p -value	VIF
Intercept	5.04	0.21	4.59-5.49	0.001	-

ARTICLE IN PRESS

FR	0.19	0.05	0.09-0.29	0.002	2.24
FL	0.06	0.02	0.02-010	0.015	1.96
W/C	-0.62	0.15	-0.93-0.31	0.001	2.58
FA/CA	0.15	0.04	0.07-0.23	0.004	1.81
(W+C)/A	-0.11	0.05	-0.21-0.01	0.041	2.02

Table 7. Regression coefficients, 95 % confidence intervals, and diagnostic statistics for the empirical model predicting flexural strength (Equation 3).

Predictor	Coefficient(β)	Std. Error	95 % Cl: (L-U)	p -value	VIF
Intercept	1.92	0.12	1.68-2.16	0.001	-
FR	0.11	0.03	0.05-0.17	0.002	2.21
FL	0.04	0.01	0.02-0.06	0.010	2.08
W/C	-0.48	0.1	-0.68-0.28	0.001	2.45
FA/CA	0.12	0.03	0.06-0.18	0.004	1.92
(W+C)/A	-0.1	0.04	-0.18-0.02	0.042	2.05

To ensure the validity and generalization of the artificial neural network (ANN) model developed to predict the compressive strength (CS), splitting tensile strength (STS), and flexural strength (FS) of concrete incorporating GFRW, a 5-fold cross-validation method, as depicted in Figure 16, was utilized. This method includes the methodical division of a dataset containing 145 unique samples, into five mutually exclusive subsets . Each fold was successively used as a validation set, while the other four folds functioned as the training data. The distribution of samples across all folds confirms that the model was exposed to a diverse representation of the dataset throughout the training and evaluation phases. Such comprehensive exposure improved the model's ability to generalize to unseen data. The model achieved low root mean square error (RMSE) values across all strength properties and fiber contents. Specifically, fold-wise RMSE values for compressive strength remained within the range of 0.06–0.15 MPa, while STS and FS showed even lower ranges of 0.005–0.032 MPa and 0.013–0.025 MPa, respectively, all comfortably below predefined engineering tolerance thresholds (0.65 MPa for CS, 0.065 MPa for STS, and 0.14 MPa for FS).

These outcomes clearly demonstrate that the ANN model exhibits high reliability and robust predictive accuracy. The cross-validation metrics confirm that the model consistently performs well across different subsets of the data, without overfitting or bias toward particular mix configurations. Therefore, the ANN model presents itself as a dependable

and effective tool for optimizing the mechanical performance of sustainable concrete composites incorporating GFRW.

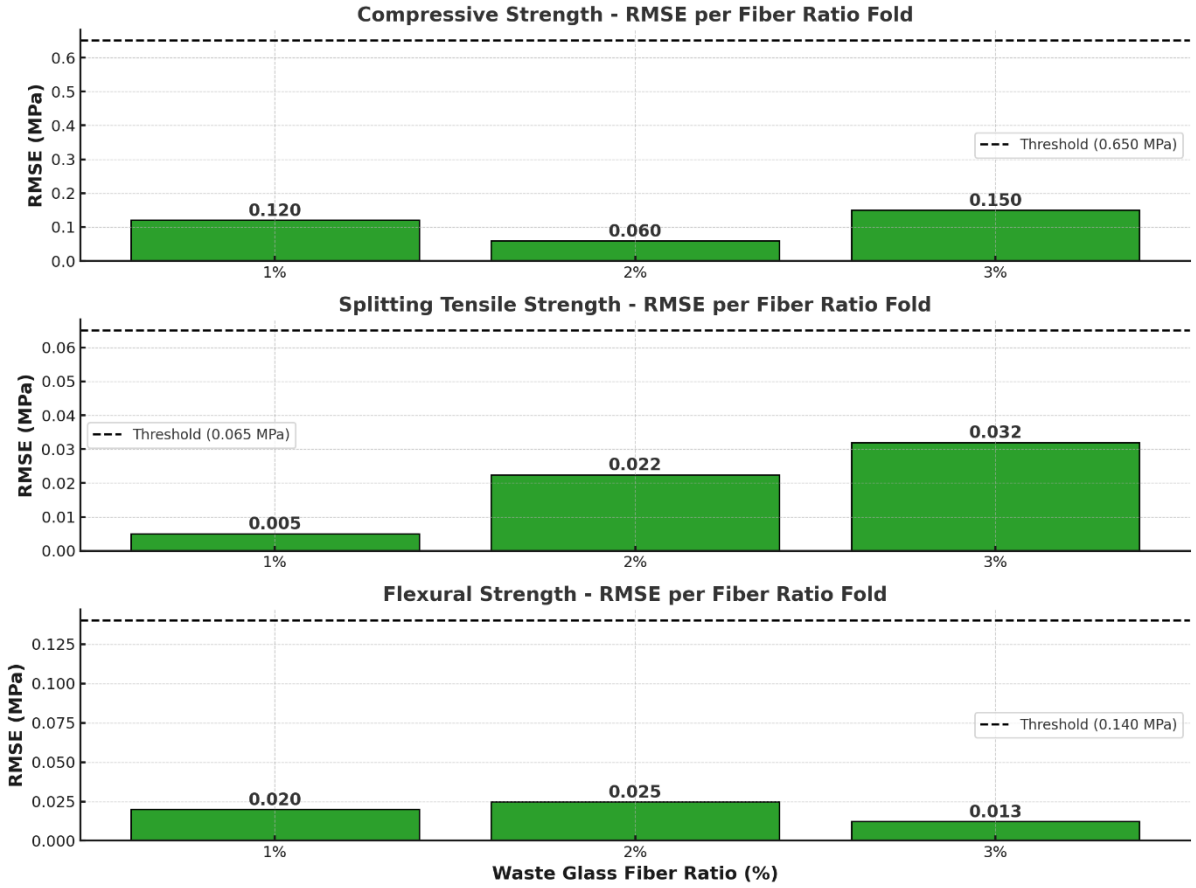


Figure 16. K-Fold validation results.

To ensure a consistent comparison between training and testing phases, all RMSE values were recalibrated to physical units (MPa). In cross-validation, normalized RMSE values ranging from 0.06 to 0.15 for compressive strength correspond to 0.36 to 0.90 MPa post-denormalization, which is consistent with the final test-set RMSE of 0.618 MPa presented in Figure 16. The denormalized fold-wise RMSE values for splitting tensile and flexural strengths range from 0.005 to 0.032 MPa and 0.052 to 0.10 MPa, respectively, which are near their final test-set errors of 0.058 MPa and 0.125 MPa. The results affirm that the model exhibits uniform predictive accuracy in both internal and external evaluation phases. Table 8 includes the per-fold performance metrics for all strength parameters, illustrating the model's consistent generalization ability across different data subsets.

Table 8: Per-fold cross-validation results for the artificial neural network (ANN) prediction of concrete strength parameters.

ARTICLE IN PRESS

Fold	RMSE (CS, MPa)	RMSE (STS, MPa)	RMSE (FS, MPa)	R^2 (CS)	R^2 (STS)	R^2 (FS)
1	0.42	0.009	0.065	0.94	0.93	0.95
2	0.50	0.012	0.070	0.95	0.94	0.96
3	0.72	0.018	0.088	0.93	0.92	0.94
4	0.36	0.006	0.052	0.96	0.95	0.97
5	0.40	0.10	0.058	0.95	0.94	0.95
Mean±SD	0.48±0.14	0.011±0.004	0.067±0.013	-	-	-

All RMSE values are presented in MPa following the denormalization of the standardized ANN outputs. The results confirm that the model attained significant predictive stability across all five folds, exhibiting minimal variance ($\sigma < 0.02$ MPa for tensile and flexural predictions). While the ANN model underwent internal validation via a five-fold cross-validation procedure, external validation with an independent experimental dataset was not conducted in this study.

The ANN model produced high predictive accuracy ($R^2 > 0.93$, RMSE < 2.0 MPa) while staying light on computation. We trained and tested it in Python with TensorFlow and Keras on a regular workstation (Intel i7 CPU, 16 GB RAM), and each cross-validation fold finished in less than a minute. The network's compact structure; two hidden layers with 12 and 8 neurons; assisted that it converge quickly and run smoothly without the need for a GPU. This efficiency makes the model straightforward to use in both research and industrial settings. The dataset contained 145 samples, so several precautions were taken to prevent the model from overfitting. We used five-fold cross-validation, L2 regularization, and early stopping to stabilize learning and keep the network from memorizing noise. The predicted and measured strengths were nearly identical across all folds, indicating that the model understood the primary nonlinear relationships between GFRW parameters and mechanical behavior. In any case, future studies should test the model on larger and more diverse datasets, such as different mix designs, curing conditions, and waste fiber types, to ensure it works and can be applied in more real-world scenarios.

To keep the ANN reliable and prevent overfitting, several precautions were built into the training process. Early stopping and dropout regularization (rate = 0.2) were implemented to ensure that training stopped automatically if the validation loss failed to improve after 30 epochs. This enabled the network to circumvent the memorization of arbitrary noise within the data. L2 regularization was incorporated to constrain the weight values within acceptable bounds and facilitate a more gradual learning process.

The trained ANN model was then used to check which input factors mattered most for predicting strength. The analysis involved changing one variable at a time within its experimental limits while keeping the others fixed, so that the effect of each could be seen clearly.

FR and FL dominated performance, shaping compressive, tensile, and flexural behavior (Figure 17). This matches fibers' physical role in crack bridging and stress transfer. The water-to-cement ratio was next because it affects matrix density and fiber bonding to paste. Although less significant, aggregate proportions-controlled workability and internal cohesion. Later-age strength improved slightly with curing time and hydration.

Altogether, the analysis confirmed that the ANN model reproduced realistic material behavior. In practical terms, mixes with roughly 1.2–1.5 % fiber content, fibers around 6 mm long, and a W/C ratio near 0.45 achieved the best balance of strength and microstructural stability.

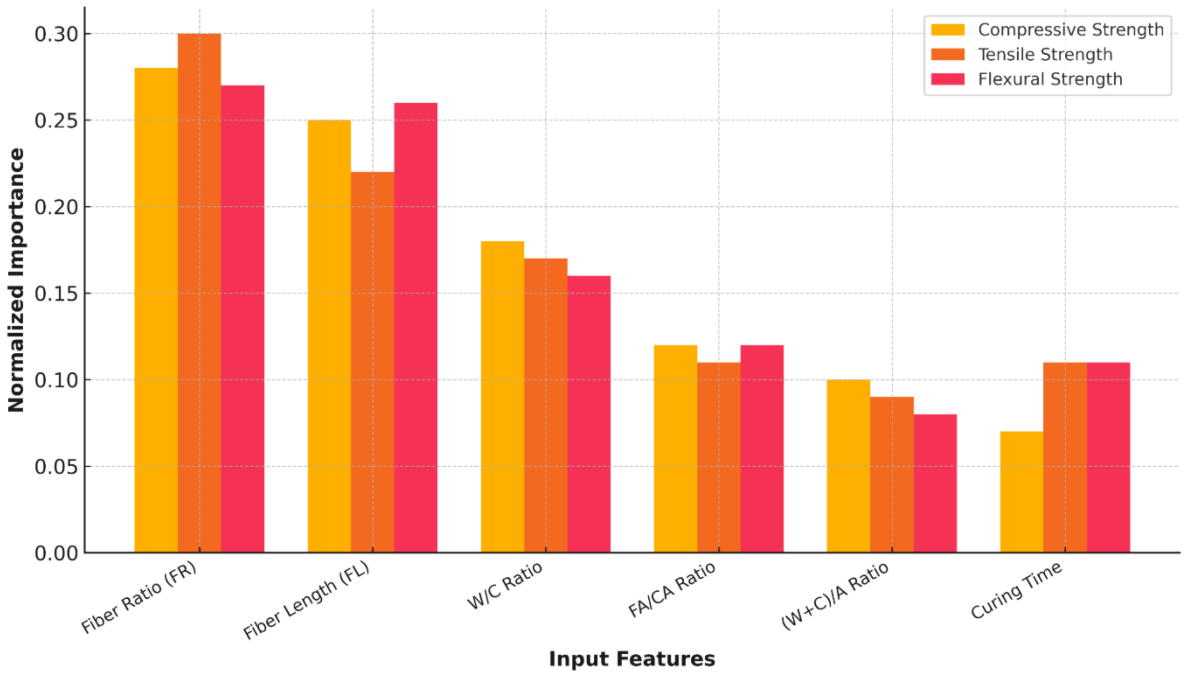


Figure 17. Feature importance analysis results.

To gain an improved understanding of the advantages of the ANN method, its predictions were compared to two common ML techniques, namely, Random Forest (RF) and Support Vector Machine (SVM). To ensure fairness, each model was trained and evaluated on the same dataset, with the same assessment criteria. The ANN performed the best, with a R^2 value of 0.93 and an RMSE of less than 2.0 MPa. The RF and SVM models came in second, with R^2 values of 0.89 and 0.86, and RMSE values of 2.7 MPa and 3.1 MPa, respectively.

These findings indicate that the ANN captured the complex and nonlinear relationships among key variables such as fiber ratio, fiber length, and water-to-cement ratio—more effectively than the other algorithms. While RF still performed reliably, it showed less sensitivity to subtle variable interactions, and SVM struggled to maintain accuracy when dealing with

ARTICLE IN PRESS

higher-dimensional, nonlinear data. Overall, the ANN model provided the most consistent and interpretable predictions, confirming its strength as a practical tool for modeling and improving the mechanical behavior of GFRW-reinforced concrete.

Alongside the machine-learning comparison, the ANN model was also tested against a conventional statistical approach; Multiple Linear Regression (MLR). The MLR model served as a baseline to judge how data-driven algorithms perform when trained on the same inputs and dataset. Although MLR was able to capture the general linear relationships between the mix variables and strength values, it could not represent the nonlinear and interaction effects caused by changes in fiber length, fiber content, or water-to-cement ratio. As a result, MLR achieved an R^2 of 0.82 and an RMSE of 4.1 MPa, which was notably lower than the ANN's accuracy (R^2 = 0.93, RMSE < 2.0 MPa).

The stronger performance of the ANN reflects its capacity to learn complex patterns and variable interactions that conventional regression methods cannot easily model. These results reinforce that machine-learning techniques; especially ANN offer a clear advantage for predicting and optimizing the behavior of GFRW-based concrete, where many factors act together in nonlinear ways.

To evaluate the efficacy of each ANN's learning from the data and to identify indications of underfitting or overfitting, the training and validation losses were monitored over 200 epochs. Figure 18 illustrates that the three models; predicting compressive, splitting tensile, and flexural strengths; exhibited distinct and consistent convergence. In all instances, the validation curve closely mirrored the training curve, both stabilizing after approximately 120 epochs, indicating that early stopping was effective in halting additional training once the model achieved optimal performance.

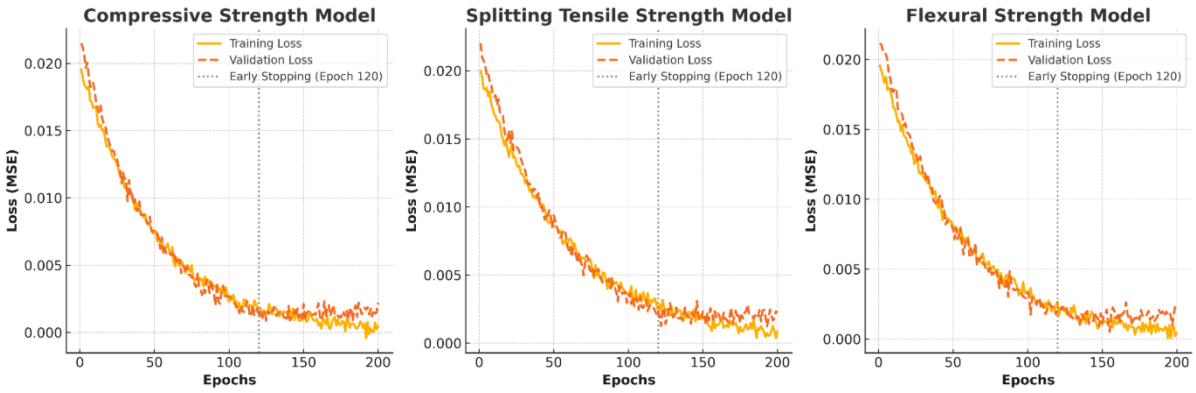


Figure 18. ANN learning curves.

ARTICLE IN PRESS

The proposed ANN framework shows strong potential for real-world use in large construction projects. With enough experimental and field data, the model could be built into decision-support tools or mix-design software to suggest the best fiber content, fiber length, and mix proportions for a given strength or durability target. This would let engineers explore many design options digitally before starting laboratory trials, helping to save time, reduce testing costs, and cut down on material waste.

The model can also be retrained or extended to include new sustainability factors, such as CO_2 emissions or the use of recycled materials, supporting the broader move toward data-driven and low-carbon construction. In practice, these capabilities help engineers and materials experts apply artificial intelligence to make better use of resources and maintain reliable performance under different environmental and operational conditions.

3.3. SEM and EDX Results

Field Emission Scanning Electron Microscopy (FE-SEM) analysis was performed to understand the microstructure of the concrete produced with glass fiber addition. The FE-SEM images in Figure 19(a) show the size and distribution of pores in the microstructure of the concrete. At the 2 µm scale, the non-compact, granular, and irregular surface morphology of the concrete concentrated within the matrix is visible prior to interaction with the fibers. Porosity has a direct effect on the mechanical strength, permeability and resistance to chemical attack. In general, capillaries appear as large, regular geometric shapes, while gel are much more irregular and smaller. High porosity causes water and harmful ions to penetrate more easily into the concrete. This can lead to concrete becoming more susceptible to corrosion and deterioration from environmental influences. The added glass fiber has the potential to reduce these disadvantages. Figure 19(b) shows the distribution of glass fibers in the concrete matrix, the interface (fiber-matrix bonding region), and the surrounding microstructure. At the 100 µm scale, roving GFRW is embedded along its long axes within the matrix, and good mechanical interlocking between the fibers and the matrix is observed at the macro level. This interlocking has a performance-enhancing effect in terms of flexural strength. The homogeneous and perpendicular distribution of glass fibers increases both the compressive and flexural strength of concrete. At the 1 µm scale in Figure 19(c), it is understood that calcium silicate hydrate (C-S-H) gel phases adhere to the fiber surface around GFRW, developing a denser microstructure. Image analysis plays an important role in understanding the properties of the material. Ettringite ($3CaO\text{-}Al_2O_3\text{-}3CaSO_4\text{-}32H_2O$) is a mineral phase formed during cement hydration, which has significant effects on the strength and volume stability of concrete. Ettringite typically appears as needle-like crystals in FE-SEM images. Needle-like crystals are present, although not very prominent here. The presence of sulfate ions, high pH, sufficient moisture,

ARTICLE IN PRESS

and aluminate components favor ettringite formation. Excess sulfate or moisture conditions can lead to delayed ettringite formation and cracking of the concrete. The absence of cracks in the image indicates that the cement hydration occurred on time and provided a good bond. Figure 19(d), at a scale of 10 µm, shows that the concrete matrix tightly accumulates around the smooth surface texture of the GFRW and strengthens the fiber-matrix interface adhesion. In areas where the fibers are very close to each other or overlap, the matrix material cannot penetrate sufficiently. This leads to a weaker and reduced bond surface. Trapped voids or pores can form between overlapping fibers. These voids disrupt the continuity of bonding and adversely affect load transfer. Good mixing, an optimum ratio, and homogeneous distribution during production are important for compressive strength. In addition, effective load transfer between fibers is ensured by strong bonding. However, if the fibers overlap and the amount of matrix between them is not sufficient, this weakens the load transfer mechanism. It can cause significant losses, especially in flexural strength.

The FE-SEM images (a–d) in Figure 19 clearly reveal the microstructural morphology of the GFRW strands used in the study and their distribution within the matrix. Images at 100 µm and 10 µm scales (b and d) show that the fibers are long-axis, cylindrical in shape and are present in the concrete matrix both as individual GFRW and as rope bundles. Higher magnification 2 µm and 1 µm scale images (a and c) reveal that C–S–H gel deposits adhere to the fiber surfaces, forming a dense binder layer at the interface, along with the distinct roughness of the fiber surfaces. These observations confirm that waste glass roving fibers have a micrometer-scale diameter range and typical roving morphology; they also demonstrate that strong adhesion develops at the fiber-matrix interface. Therefore, the FE-SEM data in Figure 19 provides sufficient qualitative confirmation of the particle size character and morphology of the fibers at the microstructural level.

ARTICLE IN PRESS

ARTICLE IN PRESS

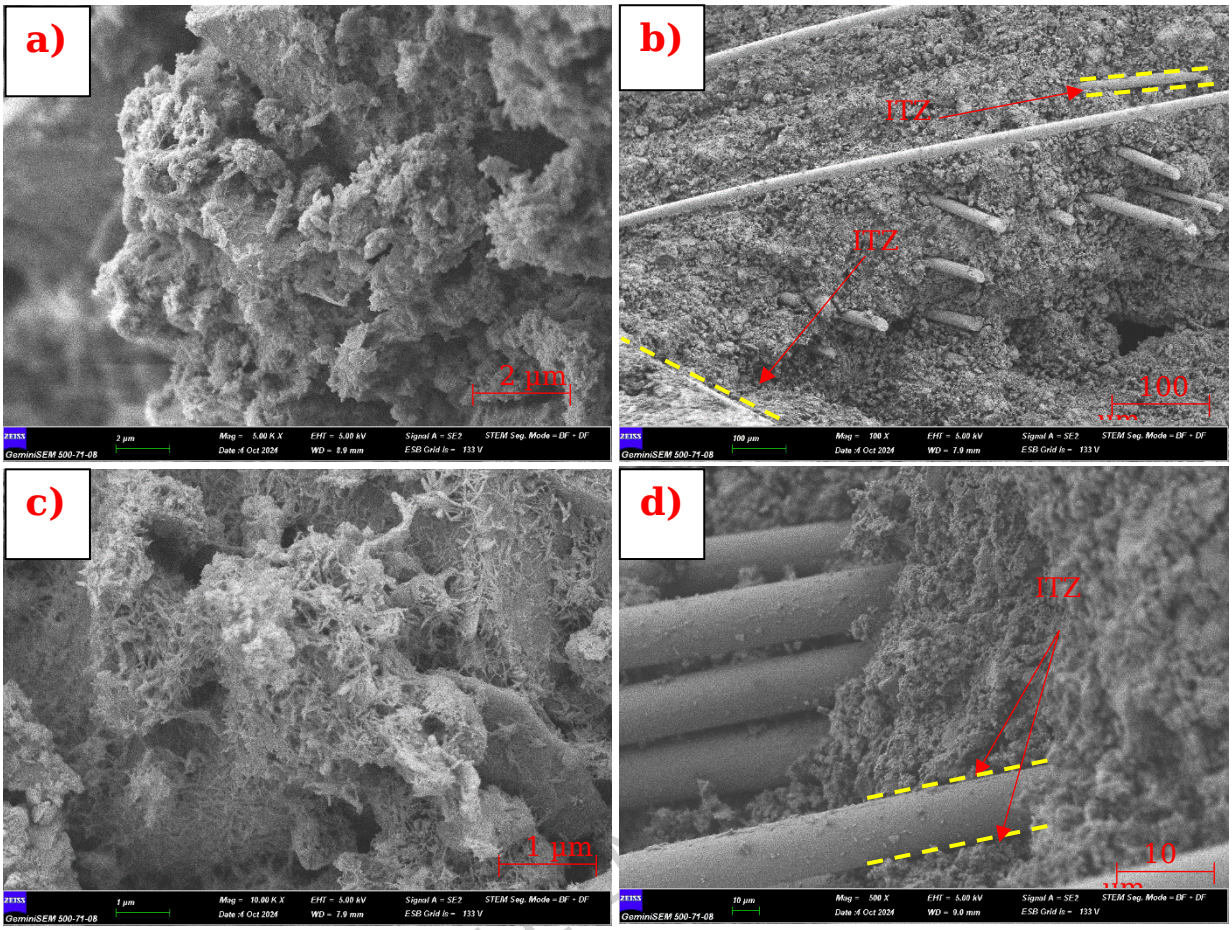


Figure 19. FE-SEM Analysis.

The incorporation of GFRW into concrete enhances its strength by improving water retention and facilitating the formation of microstructures. The fibers provide additional surfaces to the cement paste, serving as nucleation sites that facilitate the formation of hydration products, particularly at the fiber-matrix interface. The mobile filaments exhibit chemical stability and possess a substantial surface area, functioning as diminutive restraining components that mitigate the propagation of microcracks and curtail early-age shrinkage. The interfacial transition zone (ITZ) becomes denser, facilitating the transfer of stress from the paste to the surrounding aggregates.

The FE-SEM images presented in Figures 19b and 19d clearly show that a ITZ is formed between the GFRP strands and the cement mortar matrix. Figure 19b, with a medium magnification of 100 µm, shows that the fibers are embedded in the matrix with a continuous adhesion surface and that no voids or separation are observed around the fibers. In Figure 19d images, dense C–S–H gel accumulations along the rough surfaces of the glass fibers reveal that the fiber surface and cement hydration phases are integrated through chemical and mechanical bonding. Furthermore, the compact binder layer surrounding the fiber surface in Figure 19d indicates

ARTICLE IN PRESS

the formation of a strong micro-locking mechanism within the ITZ. These findings confirm that glass fiber waste acts as an effectively bonded reinforcement element rather than a physical filler in the cement matrix, supporting the results obtained in terms of mechanical strength increase from a microstructural perspective.

Chemical Composition (Weight % and Atomic % Values) of the elements as a result of EDX analysis: Oxygen (O) is 52.3% (weight) and 70.42% (atomic); the high percentage of O indicates the concentration of oxide components in the sample. This confirms that the glass fiber and matrix are in an oxide-based structure (Figure 20). Silicon (Si) is observed as being present at 12.57% by weight and 9.64% by atomic percent. Si is one of the structural components of glass fibers and can also be present in the matrix as silicate minerals or compounds. Silicate-containing binders contribute to strong mechanical properties. Calcium (Ca) is present in the structure at 27.63 weight percent and 14.85 atomic percent. A high Ca content indicates that the matrix contains a calcium-based binder. Ca excess may have an important role in matrix-fiber bonding. Aluminum (Al) is present in the structure as 3.82% (weight), 3.05% (atomic). The Al content indicates the presence of alumina or aluminum oxide phases. This can increase the strength of the matrix and promote bonding. Magnesium (Mg) was detected as 0.87% (weight) and 0.77% (atomic). The low Mg content is probably part of the matrix as an additive or trace element. Potassium (K) appears in the microstructure as 1.13% (weight), 0.62% (atomic). K can contribute to the mineral phases of the matrix or exist as a trace element. Finally, Iron (Fe) is present as 1.7% by weight; 0.66% by atomic percentage. The low proportion of Fe indicates its presence as a trace element in the fiber or matrix. It may be color or hardness contributor. The Ca, Si, and O peaks clearly observed in the EDX spectrum indicate the intensive formation of C–S–H gel, which is the main binding phase of cementitious concrete. C–S–H is the fundamental binder responsible for a large portion of the strength in cementitious systems. A high Si–Ca–O ratio indicates that more C–S–H is formed within the matrix, leading to a more compact, denser, and mechanically stiffer microstructure. This is particularly critical for a matrix reinforced with glass fiber strands. The accumulation of C–S–H gel with a high Si–Ca–O content on and around the fibers strengthens the fiber–matrix interface bond. The silica (SiO_2) structure on the surface of glass fibers is chemically compatible with cement hydrates; this compatibility facilitates C–S–H formation at the interface, enabling more efficient load transfer. Thus, the fibers better resist tensile stresses, limit the propagation of microcracks, and increase the toughness, ductility, and impact resistance of the concrete. High proportions of O, Si, and Ca indicate strong binding potential. However, the effectiveness of binding depends on the homogeneous distribution of the matrix and the presence of voids. The Ca-rich matrix has sufficient oxide phases that can form chemical bonds with

glass fibers. This can increase the charge transfer. Trace elements (Mg, Fe, K) may not have a direct effect on bonding but may contribute to the overall chemical and mechanical stability of the matrix.

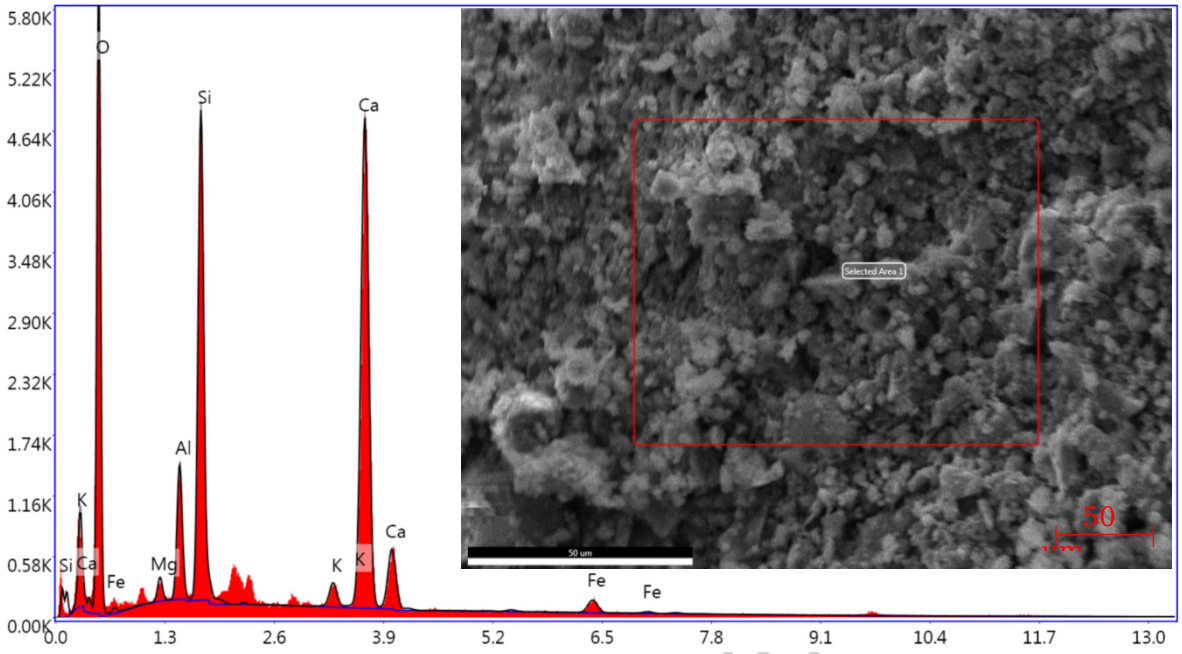


Figure 20. EDX Analysis results.

Beyond its mechanical and modeling aspects, this study also demonstrates clear environmental gains by reusing glass fiber roving waste (GFRW) in concrete production. For the fiber contents tested here (0.5–1.5 % by volume), the mixes used roughly 12–35 kg of waste per cubic meter of concrete, depending on density and fiber dosage. On a larger scale, this means that about 8–10 tons of glass fiber waste could be diverted from landfills for every 1,000 m^3 of concrete produced.

By avoiding the production of new glass fibers and reducing the need for incineration, GFRW-reinforced concrete can potentially save 18-25 kg of CO_2 per cubic meter. New glass fibers typically emit 1.6-1.8 kg of CO_2 per kilogram. For large tasks covering approximately 10,000 m^3 of material, this equates to roughly 180-250 metric tons of reduced CO_2 emissions. These estimates underscore that the reutilization of GFRW not only diverts industrial waste but also diminishes embodied carbon, thereby strengthening the argument for circular and resource-efficient methodologies in sustainable concrete design.

3.4. Study Limitations

This study provides valuable insights into the mechanical performance and predictive modeling of GFRW-reinforced concrete; however, several limitations must be acknowledged for clarity and reproducibility. The ANN model was constructed using a singular experimental dataset comprising 145 samples acquired under regulated laboratory conditions. Despite

ARTICLE IN PRESS

cross-validation demonstrating robust accuracy ($R^2 > 0.93$), the model has not been evaluated on external datasets, leaving its capacity to generalize to different mix compositions or environmental conditions indeterminate. Furthermore, the network was trained within defined ranges of water-to-cement and fiber ratios, and outcomes exceeding those parameters should be interpreted with caution.

This study primarily concentrated on mechanical performance, neglecting durability aspects such as sulfate resistance, freeze-thaw behavior, and chloride penetration. These factors are crucial for comprehending the long-term performance of GFRW concrete. Future research ought to integrate multi-institutional datasets and field-scale testing to comprehensively validate the model and investigate its potential for sustainable, long-term applications.

4. Conclusion

This study clearly demonstrates that integrating GFRW into concrete mixtures is not only an environmentally responsible solution but also a technically effective method for enhancing mechanical performance. To support and generalize these findings, an artificial neural network (ANN) model was developed and rigorously validated through a 5-fold cross-validation approach. The model demonstrated high predictive accuracy, effectively capturing the nonlinear relationships between mix design parameters and mechanical properties of the concrete.

The evaluation of the results showed that adding glass fiber roving waste (GFRW) noticeably improved the concrete's mechanical properties. The best performance was achieved with 1–2 % fiber content and a fiber length of 6 mm, which produced about 15 % higher compressive strength, 23 % higher splitting tensile strength, and 20 % higher flexural strength compared with the control mix. These gains can be linked to stronger bonding at the fiber matrix interface and the fibers' ability to bridge cracks, as seen in the SEM images.

The findings validate that the judicious application of GFRW enhances the concrete matrix and fosters sustainability by diminishing composite waste directed to landfills. The ANN model effectively captured these associations, further illustrating how data-driven techniques may enhance mix optimization for more sustainable, high-performance concrete. The main outcomes can be drawn as follows:

- Fiber length of 6 mm fibers yielded the greatest strength gains with approximately 14% in compressive strength and 13% in splitting tensile strength compared to reference concrete. On the other hand, short fiber of 3 mm provided less improvements approximately 8–10% increase strength while excessively long fibers of 9–12 mm) offered only lowest increase with approximately 1–5% strength due to poor dispersion.

ARTICLE IN PRESS

- The use of the fiber content of 1% increased the compressive and flexural strengths by approximately 10%, and splitting tensile strength by approximately 9%. On the other hand, the fiber content of 2% slightly higher gains in tensile capacity up to approximately 11.5% but only approximately 3% increase in compressive strength. However, at 3% fiber volume, strength decreased by approximately 3–5% across all tests due to fiber clumping and compromised mix homogeneity.
- Through systematic experimental analysis, it was determined that an optimal fiber length of 6 mm and a fiber ratio between 1% and 2% provide significant improvements in compressive, splitting tensile, and flexural strengths. In contrast, excessive fiber content (3%) or longer fiber lengths (9–12 mm) led to fiber agglomeration, decreased workability, and a noticeable reduction in structural performance.
- The ANN achieved coefficient of determination (R^2) values exceeding 0.93 across all three strength parameters, confirming its strong alignment with experimental data. RMSE of approximately 0.62 MPa for compressive, 0.06 MPa for splitting tensile, and 0.12 MPa for flexural strength, confirmed high precision These results confirm that the ANN was able to capture the complex, nonlinear relationships between fiber geometry, mixture ratios, and mechanical behavior with remarkable consistency and reliability.
- Moreover, microstructural (FE-SEM) and compositional (EDX) analyses validated the effective dispersion of fibers and strong fiber-matrix bonding, contributing to the observed strength improvements.
- This study validates the immediate mechanical advantages of integrating GFRW into concrete; however, it does not examine long-term performance factors, including durability against environmental exposure, freeze-thaw cycles, and chemical resistance. These variables are essential for practical applications and will be the focus of future research to thoroughly evaluate the viability and durability of GFRW-reinforced concrete over prolonged service durations.
- Although the ANN model exhibited significant predictive accuracy, it was developed using a comparatively limited experimental dataset. Despite the utilization of five-fold cross-validation and regularization to mitigate overfitting, the model's generalizability could be enhanced by integrating supplementary data. Future research should aim to augment the dataset with standardized experimental findings from additional studies involving GFRW to enhance the model's robustness.

ARTICLE IN PRESS

Future work could expand this study by exploring a wider set of machine-learning and optimization methods. Techniques such as reinforcement learning (RL) and genetic algorithms (GA) may help the model automatically find the best mix of fiber content, fiber length, and proportions to meet specific performance goals. These approaches offer strong potential for dynamic optimization, as they can gradually adjust design variables based on feedback from predicted results. Utilizing ML tools along with multi-objective optimization could also help find a better balance between cost, strength, and sustainability. Researchers can learn more about how GFRW works and get closer to designing the next generation of sustainable concretes by using these data-driven methods.

In conclusion, GFRW can be successfully repurposed into high-performance, sustainable concrete, provided that mix designs are carefully optimized. The integration of AI-based modeling tools such as ANN further enables performance prediction, reduces experimental workload, and accelerates the development of environmentally friendly construction materials. Future research should focus on long-term durability, environmental exposure scenarios, and large-scale implementation to fully realize the potential of GFRW in modern construction.

Funding: The authors extend their appreciation to the Deanship of Research and Graduate Studies at King Khalid University for funding this work through Large Research Project under grant number RGP2/601/45.

Acknowledgements: The authors extend their appreciation to the Deanship of Research and Graduate Studies at King Khalid University for funding this work through Large Research Project under grant number RGP2/601/45.

Data Availability: Data will be provided upon request from corresponding authors

Conflict of interest The authors confirm that there are no known conflicts of interest associated with this publication and there has been no significant financial support for this work that could have influenced its outcome.

Declaration of Generative AI and AI-assisted technologies in the writing process

During the preparation of this work, the authors used ChatGPT in order to improve several important aspects of writing, such as readability, grammar, spelling, and tone of the text. After using this tool, the authors

ARTICLE IN PRESS

reviewed and edited the content as needed and take full responsibility for the content of the publication.

AUTHORSHIP CREDIT STATEMENT:

Yasin Onuralp Özkılıç: Conceptualization, Methodology, Resources, Data Curation, Writing - original draft, Writing - review & editing,

Sadık Alper Yıldızel: Writing - original draft, Writing - original draft, Methodology, Formal analysis, Software

Muhannad Riyadh Alasiri: Writing - original draft, Writing - review & editing, Data Curation, Funding Acqusition

Ali İhsan Çelik: Writing - original draft, Writing - review & editing, Data Curation, Formal analysis

Mohamed Abdikarin Mohamud: Writing - original draft, Writing - review & editing, Investigation

References

[1] Qsymah A, Arbili MM, Ahmad J, Alogla SM, Alawi Al-Sodani KA, Hakamy A et al. Thermal properties, microstructure analysis, and environmental benefits of basalt fiber reinforced concrete. 2023;18:15589250221146547.
[2] Pham TM. Fibre-reinforced concrete: State-of-the-art-review on bridging mechanism, mechanical properties, durability, and eco-economic analysis. Case Studies in Construction Materials. 2025:e04574.
[3] Özkılıç' YO, Beskopylny AN, Stel'makh SA, Shcherban' EM, Mailyan LR, Meskhi B et al. Lightweight expanded-clay fiber concrete with improved characteristics reinforced with short natural fibers. Case Studies in Construction Materials. 2023;19:e02367.
[4] Almeshal I, Özkılıç YO, Aksoylu C, Karalar M, Alharthai M. Ductility and strength of reinforced concrete beams strengthened with aluminum CNC waste. Structural Concrete. 2024;25:3232-45.
[5] Bertelsen IMG, Ottosen LM, Fischer G. Influence of fibre characteristics on plastic shrinkage cracking in cement-based materials: A review. Construction and Building Materials. 2020;230:116769.
[6] Hassan HZ, Saeed NM. Fiber reinforced concrete: a state of the art. Discover Materials. 2024;4:101.
[7] Ravichandran D, Prem PR, Kaliyavaradhan SK, Ambily PS. Influence of fibers on fresh and hardened properties of Ultra High Performance Concrete (UHPC)—A review. Journal of Building Engineering. 2022;57:104922.
[8] Dawood ET, Hamad AJ. Toughness behaviour of high-performance lightweight foamed concrete reinforced with hybrid fibres. Structural concrete. 2015;16:496-507.
[9] Chen Y, Waheed MS, Iqbal S, Rizwan M, Room S. Durability Properties of Macro-Polypropylene Fiber Reinforced Self-Compacting Concrete. 2024;17:284.

ARTICLE IN PRESS

[10] Latifi MR, Öznur B, and Mardani Aghabaglou A. Effect of the addition of polypropylene fiber on concrete properties. Journal of Adhesion Science and Technology. 2022;36:345-69.
[11] Amudhavalli NK, Harihanandh M. Study on strength and durability characteristics of polypropylene fiber reinforced blended concrete tiles. Int J Eng Technol. 2018;7:1544-7.
[12] Wang XQ, Chow CL, Lau D. Multiscale perspectives for advancing sustainability in fiber reinforced ultra-high performance concrete. npj Materials Sustainability. 2024;2:13.
[13] Hao H, Bi K, Chen W, Pham TM, Li J. Towards next generation design of sustainable, durable, multi-hazard resistant, resilient, and smart civil engineering structures. Engineering Structures. 2023;277:115477.
[14] Araújo EM, Araújo KD, Pereira OD, Ribeiro PC, de Melo TJA. Fiberglass wastes/polyester resin composites: mechanical properties and water sorption. Polímeros. 2006;16:332-5.
[15] Quadrini F, Bellisario D, Santo L. Molding articles made of 100% recycled fiberglass. Journal of Composite Materials. 2016;50:2959-69.
[16] Torres A, De Marco I, Caballero BM, Laresgoiti MF, Chomón MJ, Kondra G. Recycling of the solid residue obtained from the pyrolysis of fiberglass polyester sheet molding compound. Advances in Polymer Technology: Journal of the Polymer Processing Institute. 2009;28:141-9.
[17] Khan A, Khattak MJ, Pesacreta TC, Hume LA. Microstructural, mechanical, and durability assessment of sustainable geopolymers synthesized using rice husk ash, a byproduct of the rice industry. Journal of Sustainable Cement-Based Materials. 2025;14:2519-36.
[18] Khan A. Development of Green Construction Materials Using High-Content Sugarcane Bagasse Ash. 2025.
[19] Liu Y, Dong J, Yuan S, Li K, Hu X, Wang Q. Variable fatigue loading effects on corrugated steel box girders with recycled concrete. Journal of Constructional Steel Research. 2024;215:108526.
[20] Haq IU, Elahi A, Khan A, Ali A, Imran Latif Qureshi QBa, Rezzoug A et al. The addition of natural clay and industrial and agricultural waste on the performance of green and sustainable concrete. Scientific Reports. 2025;15:17034.
[21] Zhong A, Xie C, Zhang D, Gou B, Zhou J, Yu S et al. Rational design of glass fiber reinforced epoxy resin with thermal conductivity but electrical insulation through a multi-level network. Composites Communications. 2025;54:102288.
[22] Xu M-x, Ji H-w, Wu Y-c, Meng X-x, Di J-y, Yang J et al. Recovering glass fibers from waste wind turbine blades: Recycling methods, fiber properties, and potential utilization. Renewable and Sustainable Energy Reviews. 2024;202:114690.
[23] Çelik Aİ, Karalar M, Aksoylu C, Mydin MAO, Althaqafi E, Yılmaz F et al. Effect of GBFS ratio and recycled steel tire wire on the mechanical and microstructural properties of geopolymer concrete under ambient and oven curing conditions. Case Studies in Construction Materials. 2024;21:e03890.
[24] Ostrowski KA, Piechaczek M, Lach M, Sikora O, Furtak K, Sajdak K et al. Sustainable Approach to Utilization of Waste Glass Fibers and Basalt

ARTICLE IN PRESS

ARTICLE IN PRESS

Powder as Potential Additives in Epoxy-Based Composites for Reparation of Concrete Structures. Sustainability. 2025;17:1064.
[25] Zhang F, Lu Z, Wang D. Working and mechanical properties of waste glass fiber reinforced self-compacting recycled concrete. Construction and Building Materials. 2024;439:137172.
[26] Yildizel SA, Özkılıç YO, Yavuz A. Optimization of waste tyre steel fiber and rubber added foam concretes using Taguchi method and artificial neural networks. Elsevier. p. 106098.
[27] Ali B, Qureshi LA. Influence of glass fibers on mechanical and durability performance of concrete with recycled aggregates. Construction and Building Materials. 2019;228:116783.
[28] Chen Y, He Q, Liang X, Jiang R, Li H. Experimental investigation on mechanical properties of glass fiber reinforced recycled aggregate concrete under uniaxial cyclic compression. Cleaner Materials. 2022;6:100164.
[29] Celik AI, Özkiliç YO. Lightweight geopolymer concrete using pumice and glass fiber. Computers and Concrete. 2024;34:577.
[30] Sathiparan N. Innovative use of corncob ash in concrete: a machine learning perspective on compressive strength prediction. Innovative Infrastructure Solutions. 2025;10:73.
[31] Sathiparan N. Predicting compressive strength in cement mortar: The impact of fly ash composition through machine learning. Sustainable Chemistry and Pharmacy. 2025;43:101915.
[32] Sathiparan N. Prediction model for compressive strength of rice husk ash blended sandcrete blocks using a machine learning models. Asian Journal of Civil Engineering. 2024;25:4745-58.
[33] Ikumi T, Galeote E, Pujadas P, De La Fuente A, López-Carreño RD. Neural network-aided prediction of post-cracking tensile strength of fibre-reinforced concrete. Computers & Structures. 2021;256:106640.
[34] Karthiyaini S, Senthamaraikannan K, Priyadarshini J, Gupta K, Shanmugasundaram M. Prediction of mechanical strength of fiber admixed concrete using multiple regression analysis and artificial neural network. Advances in Materials Science and Engineering. 2019;2019:4654070.
[35] Mashhadban H, Kutanaei SS, Sayarinejad MA. Prediction and modeling of mechanical properties in fiber reinforced self-compacting concrete using particle swarm optimization algorithm and artificial neural network. Construction and Building Materials. 2016;119:277-87.
[36] Haigh R, Sandanayake M, Joseph P, Yaghoubi E, Vrcelj Z. The mechanical and microstructural performance of waste textile and cardboard materials in concrete. Structural Concrete. 2024;25:4033-47.
[37] Cui S, Wang T, Zhang Z, Sun X, Li J, Li B et al. Frost resistance and life prediction of recycled brick aggregate concrete with waste polypropylene fiber. 2023;62.
[38] De Silva S, Prasanthan T. Application of recycled PET fibers for concrete floors. Engineer: Journal of the Institution of Engineers, Sri Lanka. 2019;52.
[39] Samadi M, Murali G, Wong LS, Din NM, Abdulkadir I, Abdellatief M et al. Mechanical and mineralogical performance of sustainable cement composites with calcined palm oil leaf and calcined pine leaf Ash as supplementary cementitious materials. Scientific Reports. 2025;15:32610.

ARTICLE IN PRESS

[40] Abdellatief M, Elsafi M, Murali G, ElNemr A. Comparative evaluation of hybrid machine learning models for predicting the strength of metakaolin-based geopolymer concrete enhanced with Gaussian noise augmentation. Journal of Building Engineering. 2025;111:113302.
[41] Cai H, Ye J, Wang Y, Shi Y, Saafi M, Ye J. Microscopic failure characteristics and critical length of short glass fiber reinforced composites. Composites Part B: Engineering. 2023;266:110973.
[42] Yildizel SA, Tayeh BA, Calis G. Experimental and modelling study of mixture design optimisation of glass fibre-reinforced concrete with combined utilisation of Taguchi and Extreme Vertices Design Techniques. Journal of Materials Research and Technology. 2020;9:2093-106.
[43] Gao Y, De Schutter G, Ye G, Tan Z, Wu K. The ITZ microstructure, thickness and porosity in blended cementitious composite: Effects of curing age, water to binder ratio and aggregate content. Composites Part B: Engineering. 2014;60:1-13.
[44] Wu C, He X, Zhao X, He L, Song Y, Zhang X. Effect of fiber content on mechanical properties and microstructural characteristics of alkali resistant glass fiber reinforced concrete. Advances in Materials Science and Engineering. 2022;2022:1531570.
[45] Ahmad J, González-Lezcano RA, Majdi A, Ben Kahla N, Deifalla AF, El-Shorbagy MA. Glass Fibers Reinforced Concrete: Overview on Mechanical, Durability and Microstructure Analysis. 2022;15:5111.
[46] Atmakuri A, Palevicius A, Vilkauskas A, Janusas G. Numerical and Experimental Analysis of Mechanical Properties of Natural-Fiber-Reinforced Hybrid Polymer Composites and the Effect on Matrix Material. 2022;14:2612.
[47] Lin K, Wang Z. Multiscale mechanics and molecular dynamics simulations of the durability of fiber-reinforced polymer composites. Communications Materials. 2023;4:66.
[48] Kaleel I, J. PE, and Bednarcyk BA. Micromechanical modeling of discontinuous long fiber reinforced composites. Mechanics of Advanced Materials and Structures. 2025;32:596-604.
[49] Bao S, Wang S, Xia H, Liu K, Tang X, Jin P. Enhancing the Mechanical Properties of Recycled Aggregate Concrete: A Comparative Study of Basalt- and Glass-Fiber Reinforcements. 2025;15:1718.
[50] Mudi C, Shaw A. Natural fiber reinforcement-investigating ramie in cementitious composites with emphasis on fiber surface modifications. Journal of Building Engineering. 2025;100:111705.
[51] Lee M-G, Wang W-C, Wang Y-C, Hsieh Y-C, Lin Y-C. Mechanical Properties of High-Strength Pervious Concrete with Steel Fiber or Glass Fiber. Buildings2022.
[52] Tao Y, Hadigheh SA, Wang Z. Void geometry analysis and multifaceted characterisation of cementitious mortar reinforced with short carbon and glass fibres – A comparative study. Journal of Building Engineering. 2024;89:109283.
[53] Aydın S. Effects of fiber strength on fracture characteristics of normal and high strength concrete. Periodica Polytechnica Civil Engineering. 2013;57:191–200.

ARTICLE IN PRESS

[54] Pakravan HR, Memariyan F. Modification of Low-surface Energy Fibers used as Reinforcement in Cementitious Composites: A Review. Polymer-Plastics Technology and Engineering. 2017;56:227-39.
[55] Rao GA. Generalization of Abrams' law for cement mortars. Cement and Concrete Research. 2001;31:495-502.
[56] Pichler B, Hellmich C, Eberhardsteiner J, Wasserbauer J, Termkhajornkit P, Barbarulo R et al. Effect of gel–space ratio and microstructure on strength of hydrating cementitious materials: An engineering micromechanics approach. Cement and Concrete Research. 2013;45:55-68.
[57] Falliano D, De Domenico D, Ricciardi G, Gugliandolo E. Compressive and flexural strength of fiber-reinforced foamed concrete: Effect of fiber content, curing conditions and dry density. Construction and Building Materials. 2019;198:479-93.
[58] Damanik WS, Siregar MA, Lubis S. Evaluation of the effect of variations in resin and fiber composition on tensile and compressive properties of natural material composites. Hybrid Advances. 2025;10:100434.
[59] Afroughsabet V, Biolzi L, Ozbakkaloglu T. High-performance fiber-reinforced concrete: a review. Journal of Materials Science. 2016;51:6517-51.
[60] Abdellatief M, Abd-Elmaboud ME, Mortagi M, Saqr AM. A convolutional neural network-based deep learning approach for predicting surface chloride concentration of concrete in marine tidal zones. Scientific Reports. 2025;15:27611.

ARTICLE IN PRESS